AD-A226 454

ARI-RR-798

EXPERIMENTAL SUPPORT FOR AND ANALYSIS OF INFRARED EMISSION DATA FROM SOLID PROPELLANT COMBUSTION TESTS

Prepared by

K.D. Annen and J. Wormhoudt
Aerodyne Research, Inc.
45 Manning Road
Billerica, MA 01821

Prepared for

Dr. Gabriel Roy
Office of Naval Research
Arlington, VA 22217-5000

DTIC
ELECTE
SEP 07 1990
S E D

August 1990

DISTRIBUTION STATEMENT A
Approved for public release;
Distribution Unlimited

90 09 07 059

REPORT DOCUMENTATION PAGE

Form Approved
OMB No. 0704-0188

Public reporting burden for this collection of information is estimated to average 1 hour per response, including the time for reviewing instructions, searching existing data sources, gathering and maintaining the data needed, and completing and reviewing the collection of information. Send comments regarding this burden estimate or any other aspect of this collection of information, including suggestions for reducing this burden, to Washington Headquarters Services, Directorate for Information Operations and Reports, 1215 Jefferson Davis Highway, Suite 1204, Arlington, VA 22202-4302, and to the Office of Management and Budget, Paperwork Reduction Project (0704-0188), Washington, DC 20503.

1. AGENCY USE ONLY (Leave blank)	2. REPORT DATE	3. REPORT TYPE AND DATES COVERED
	31 Aug 90	Final 1 Jul 88 - 30 June 90

4. TITLE AND SUBTITLE

Experimental Support for and Analysis of Infrared Emission Data from Solid Propellant Combustion Tests

5. FUNDING NUMBERS

C N00014-88-C-0492

6. AUTHOR(S)

K.D. Annen and J. Wormhoudt

7. PERFORMING ORGANIZATION NAME(S) AND ADDRESS(ES)

Aerodyne Research, Inc.
45 Manning Road
Billerica, MA 01821

8. PERFORMING ORGANIZATION REPORT NUMBER

ARI-RR-798

9. SPONSORING/MONITORING AGENCY NAME(S) AND ADDRESS(ES)

Office of Naval Research
Arlington, VA 22217-5000

10. SPONSORING/MONITORING AGENCY REPORT NUMBER

11. SUPPLEMENTARY NOTES

12a. DISTRIBUTION/AVAILABILITY STATEMENT

Approved for public release;
distribution unlimited.

12b. DISTRIBUTION CODE

13. ABSTRACT *(Maximum 200 words)*

The objective of this program was to analyze infrared emission spectra from solid propellant combustion to obtain a better understanding of the chemical, physical, and radiative processes occurring in these flames. The spectra analyzed were obtained in the High Pressure Combustion Laboratory of the Pennsylvania State University using an infrared spectrometer and a strand burner. Comparing measured data with predictive models for emission from a substantial number of molecules whose radiative properties are well known allows determination of temperature and species concentrations in flame hot regions. Observed spectra can also be analyzed to yield radiative parameters for less well known radiators.

14. SUBJECT TERMS

Propellants, Combustion, Flames, Infrared Spectrometers

15. NUMBER OF PAGES

67

16. PRICE CODE

17. SECURITY CLASSIFICATION OF REPORT	18. SECURITY CLASSIFICATION OF THIS PAGE	19. SECURITY CLASSIFICATION OF ABSTRACT	20. LIMITATION OF ABSTRACT
Unclassified	Unclassified	Unclassified	

SUMMARY

The objective of this program was to analyze infrared emission spectra from solid propellant combustion to obtain a better understanding of the chemical, physical, and radiative processes occurring in these flames. The spectra analyzed were obtained in the High Pressure Combustion Laboratory of the Pennsylvania State University using an infrared spectrometer and a strand burner. Comparing measured data with predictive models for emission from a substantial number of molecules whose radiative properties are well known allows determination of temperature and species concentrations in flame hot regions. Observed spectra can also be analyzed to yield radiative parameters for less well known radiators.

Preliminary work included estimates of flowfield parameters, detailed chemical kinetics calculations to track conversion of initial decomposition products, and construction of line and band radiation models for several molecules. Analysis of observed spectra began with an inspection to determine what molecules contributed spectral features. Several techniques were evaluated which used spectral features to evaluate hot region temperatures. These included using the widths of CO_2 and H_2O bands, the strength ratios of low resolution H_2O bands, and the peak intensities of resolved lines in HCl and HF bands. Relative concentrations were derived for several combustion product molecules which were in accord with propellant compositions.

Accession For
NTIS GRA&I
DTIC TAB
Unannounced
Justification
By
Distribution/
Availability Codes
Dist | Avail and/or Special
A-1

TABLE OF CONTENTS

LIST OF ILLUSTRATIONS

LIST OF ILLUSTRATIONS (Continued)

1. INTRODUCTION

This is the final report for Contract N00014-88-C-0492, "Experimental Support for and Analysis of Infrared Emission Data from Solid Propellant Combustion Tests." The objective of this program was to analyze infrared (IR) emission from solid propellant combustion to obtain a better understanding of the chemical, physical, and radiative processes occurring in the combustion process. We were indeed able to demonstrate that flame temperatures and species concentrations can be obtained from infrared emission and absorption spectra.

Data analyzed under this contract were obtained in the High Pressure Combustion Laboratory of the Mechanical Engineering Department of the Pennsylvania State University, under the supervision of Profs. S.T. Thynell and K.K. Kuo. Spectra were taken using a Fourier transform infrared (FTIR) spectrometer of propellant strands burned in a chamber which allowed optical access for infrared emission and absorption measurements as well as video records of the burns.

Our work in this program was intended to enhance and complement the Penn State effort. Our focus was the analysis of the spectral data taken in the Penn State strand burner, which only became operational towards the end of the period of performance. Our work prior to the data analysis phase included some analysis of the expected flow fields in the strand burner, a few detailed computer calculations of the oxidation chemical kinetics of initial propellant decomposition products, and the development of molecular line and band models for several molecules observed in the strand burner spectra. We also delivered a copy of the computer code we use to predict emission spectra, the Aerodyne Radiation Code (ARC) to Prof. Thynell so the Penn State group could build up their own analysis capability.

The major application of solid propellants has been and continues to be in the propulsion of a wide variety of missiles. Propellant development has long focused on improved performance (specific impulse), but more recently increased emphasis has been placed on other attributes including safety and decreased detectability (low infrared emission, low contrail formation, and so forth). Furthermore, increasing consideration is being given to the use of solid propellants in advanced decoy devices. Here the goal is the opposite of that in missile propulsion- instead of minimizing the radiation signature, it should be maximized, and resemble that of the object (such as an aircraft) it protects as closely as possible.

Continued design advances in solid propellants and combustors for both these applications will come in part from a better understanding of the molecular and fluid dynamic processes in propellant combustion. IR emission is one of the few simple, widely applicable, and nonintrusive methods of obtaining basic information about propellant combustion. In addition, IR emission from the products of combustion of solid propellants also has considerable military significance. Both the initial combustion products and the products of the secondary combustion (afterburning) which occurs when the initial products mix with the atmosphere are important contributors to the total IR emission of a rocket exhaust plume or decoy flare.

Presently, a major focus of propellant development for both propulsion and decoy applications is the inclusion of boron particles. More experimental work is needed both to understand the mechanisms of boron particle combustion and to characterize the radiative properties of the molecular and particulate combustion products. The strand burner/FTIR spectrometer system at Penn State could contribute in both these areas, and indeed a boron-containing propellant was one of those first observed. However, our analysis of the spectra obtained to date not only shows that the spectra contain no observable boron molecular emission features, but that the flame temperature is such that boron

particle combustion does not occur, in agreement with the visible appearance of the flames. Nevertheless, the flame characterization capabilities which we demonstrate here using the first Penn State spectra will be valuable when propellants are burned under conditions where boron combustion does occur.

2. DATA REVIEW AND PRELIMINARY ANALYSIS OF SPECTRA

This report will focus on six emission spectra sent to us by Penn State on floppy disks in a format readable by SpectraCalc, the data processing program available on Aerodyne personal computers. The ability to further manipulate the spectral data on our computers was helpful and sometimes even necessary to our analysis work. Some earlier spectra were provided to us in hard copy only, including both absorption and emission spectra. They were not analyzed in detail, although they appear not to contain any additional information about the two propellants discussed in this report.

Figure 1 shows the transparent, low pressure strand burner used in the Penn State observations, as it was configured for the first spectra taken. Initially, the field of view of the spectrometer was centered 1 to 2 cm above the burning surface, and apertures of 0.625 or 1.875 cm diameters could be used, so that the burning surface and the hottest region of flame above it were visible. The apparatus has a highly accurate height positioning mechanism which allows the field of view of the FTIR spectrometer to remain at a constant height with respect to the burning surface during the entire test. The solid propellant sample holder is mounted on a perforated plate which allows purge gas to flow parallel to the axis of the propellant strand.

Each emission spectrum considered here is based on the co-addition of 10 separate spectra supplied to us individually. Also provided on floppy disk were a background spectrum, numbered B12001, and a response function spectrum, IRF010. The latter is a spectrum of a 1273 K blackbody divided by the spectral blackbody emission function, which has the units of $W/cm^2/sr/cm^{-1}$.

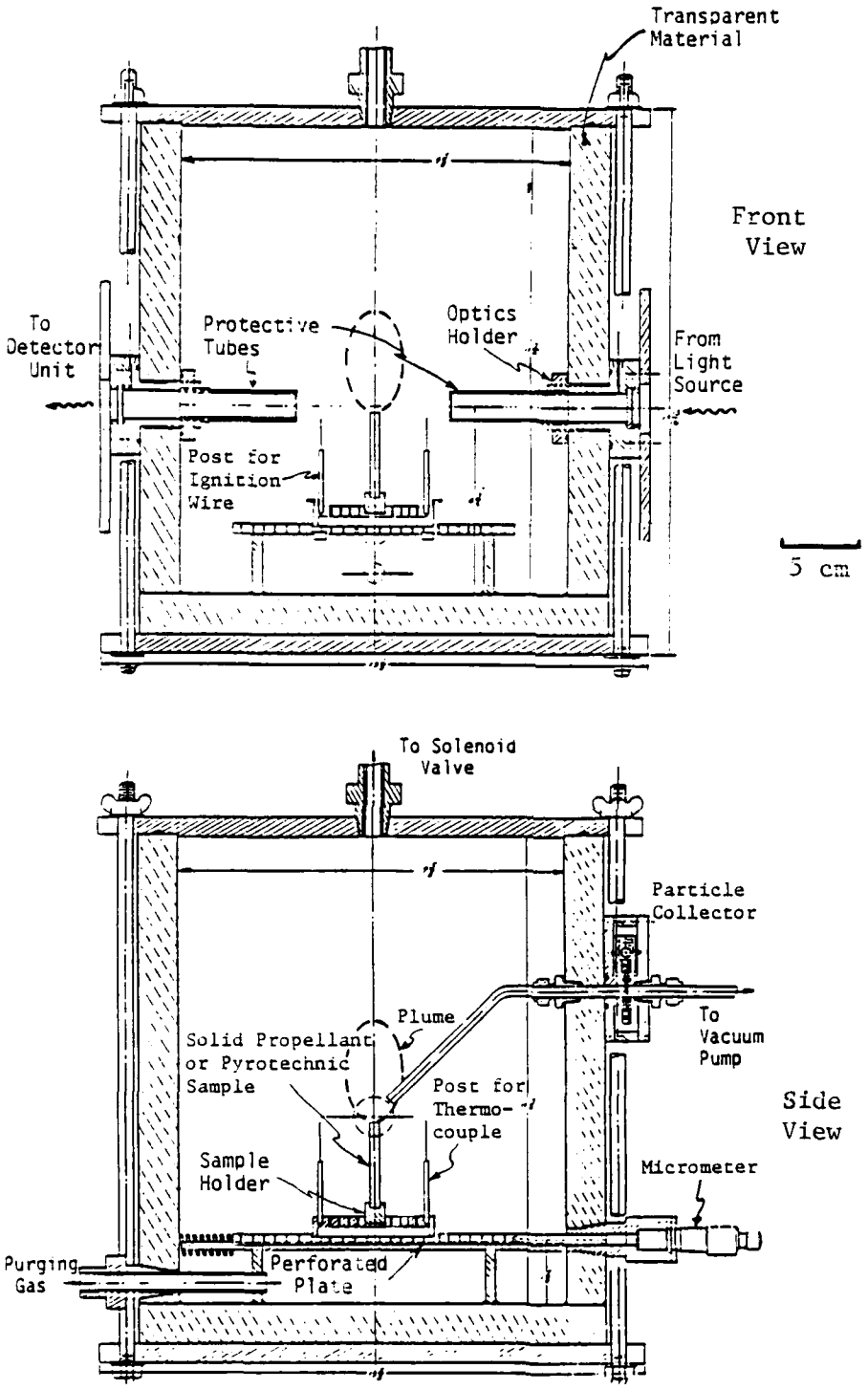

Figure 1. Penn State Transparent Strand Burner for Infrared Radiation Measurements.

The procedure used here was to subtract the background spectrum from the co-added emission spectrum, then divide by the response function. Therefore, except for changes in instrument sensitivity, the spectra displayed here should have the units of $W/cm^2/sr/cm^{-1}$ as well.

The six spectra are first displayed at their observed 4 cm^{-1} resolution in Figures 2 through 7. In Figures 2 and 3, spectra given the series numbers E12 and E13 are of NOSOL-363, a double-base propellant, burning in 5 psig of nitrogen. These are the only inert-atmosphere runs considered here, with the last four all being burns in air. Figures 4 and 5 (spectra S23 and S24) are spectra of NOSOL-363, and Figures 6 and 7 (spectra S25 and S26) of a highly energetic copolymer of BAMO/NMMO containing 5% boron.

In the following subsections we will analyze some of the spectral features in more detail. First, we make some general remarks, beginning by noting some differences in the collection parameters between spectra. E13 is seen to have less continuum (hot blackbody) contribution, which may be due to a field of view centered further above the burning surface or to the use of the smaller aperture. Similarly, S24 has a much lower continuum component than S23, here definitely because the S24 field of view was 1 cm higher. Finally, S25 shows the effects of absorption by cool, recirculating exhaust gases. In S26, plexiglass shields were placed around the burning strand and the purging of the observation region is clearly much more effective.

A number of the sharp features seen in the spectra are not individual vibrational-rotational lines but groups of lines. However, the individual lines of the HCl and HF bands are fully resolved, and those of the CO band partially resolved, as will be discussed below. In comparing with tabulated values, we saw that line positions in the Penn State spectra appear about 2.6 cm^{-1} higher in frequency than literature line positions corrected for the refractive index of air.

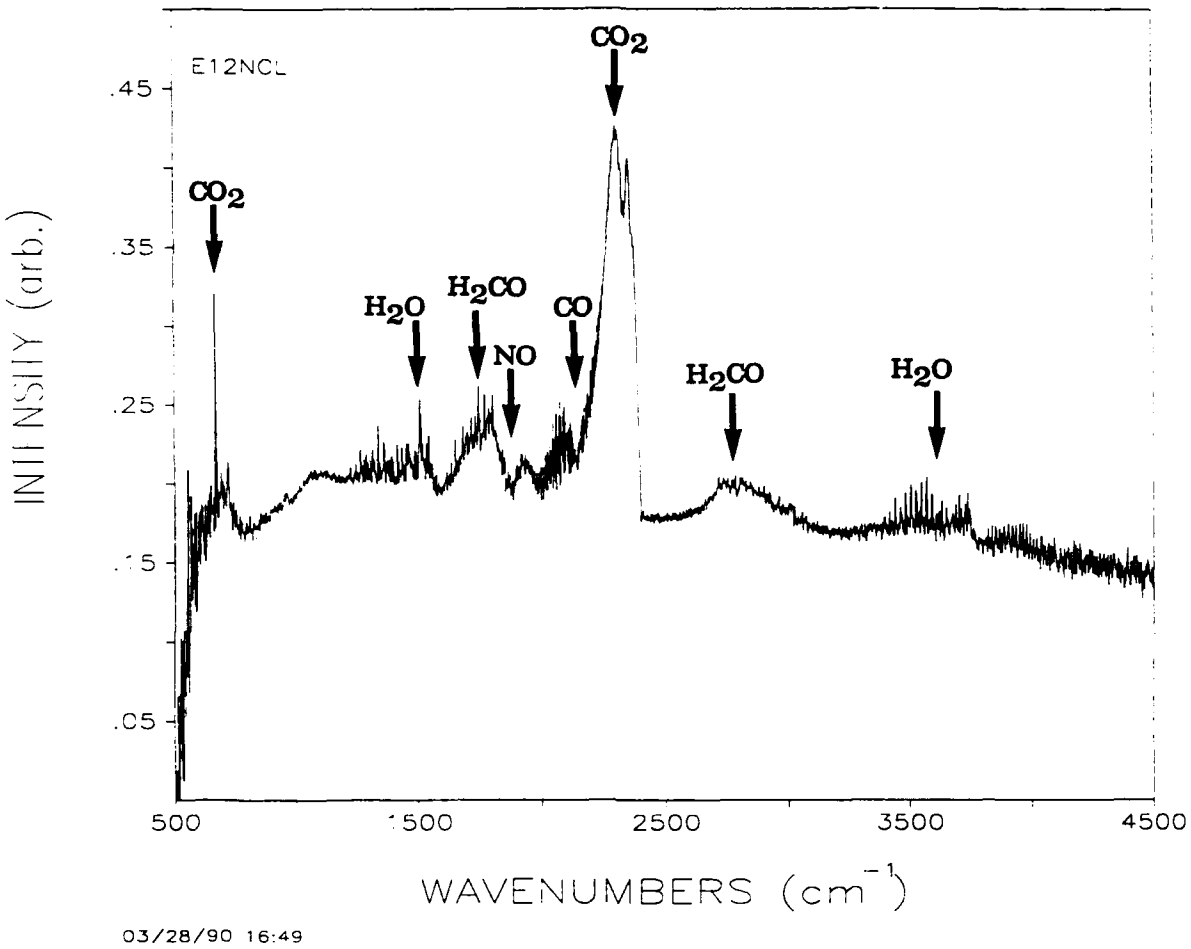

Figure 2. Penn State 4 cm^{-1} Resolution Emission Spectrum of NOSOL-363 Burning in a Nitrogen Atmosphere.

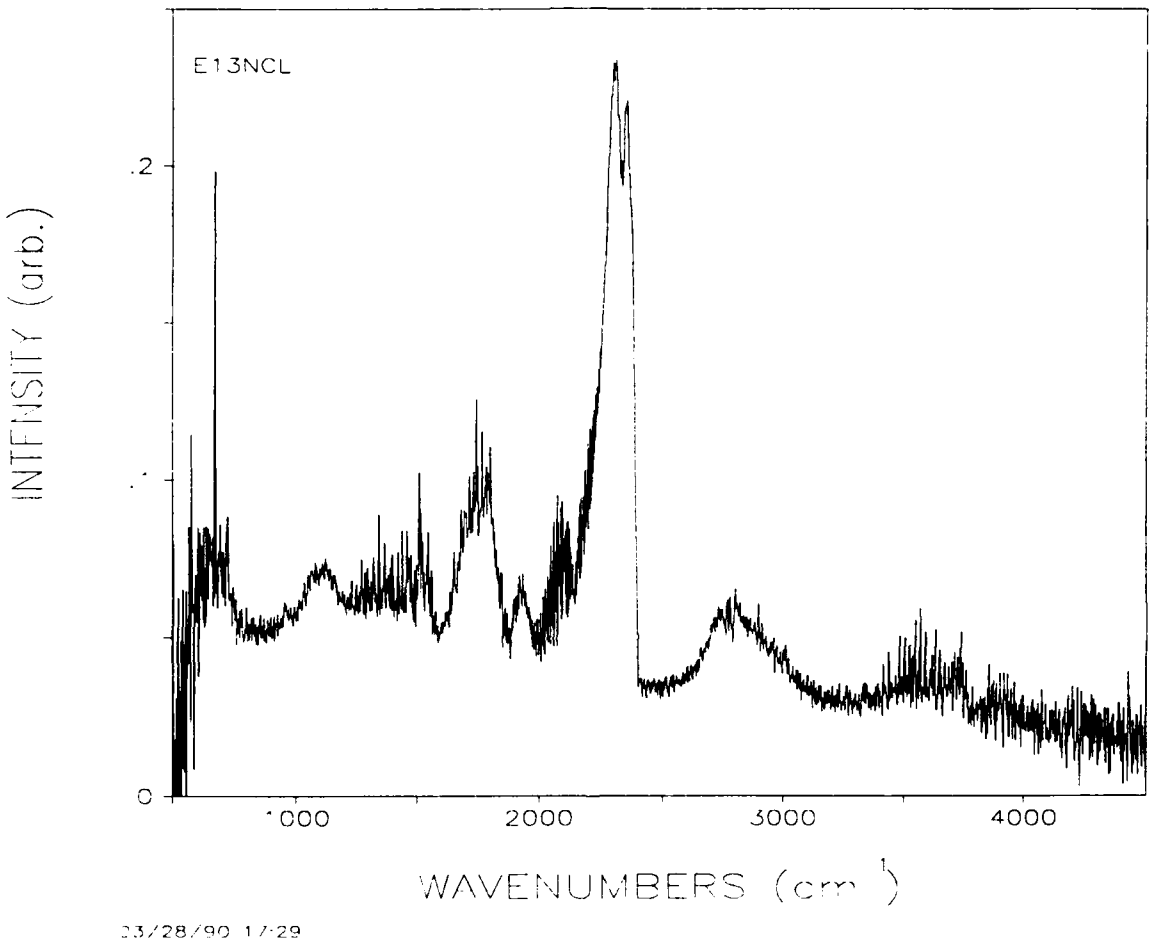

Figure 3. Penn State 4 cm^{-1} Resolution Emission Spectrum of NOSOL-363 Burning in a Nitrogen Atmosphere.

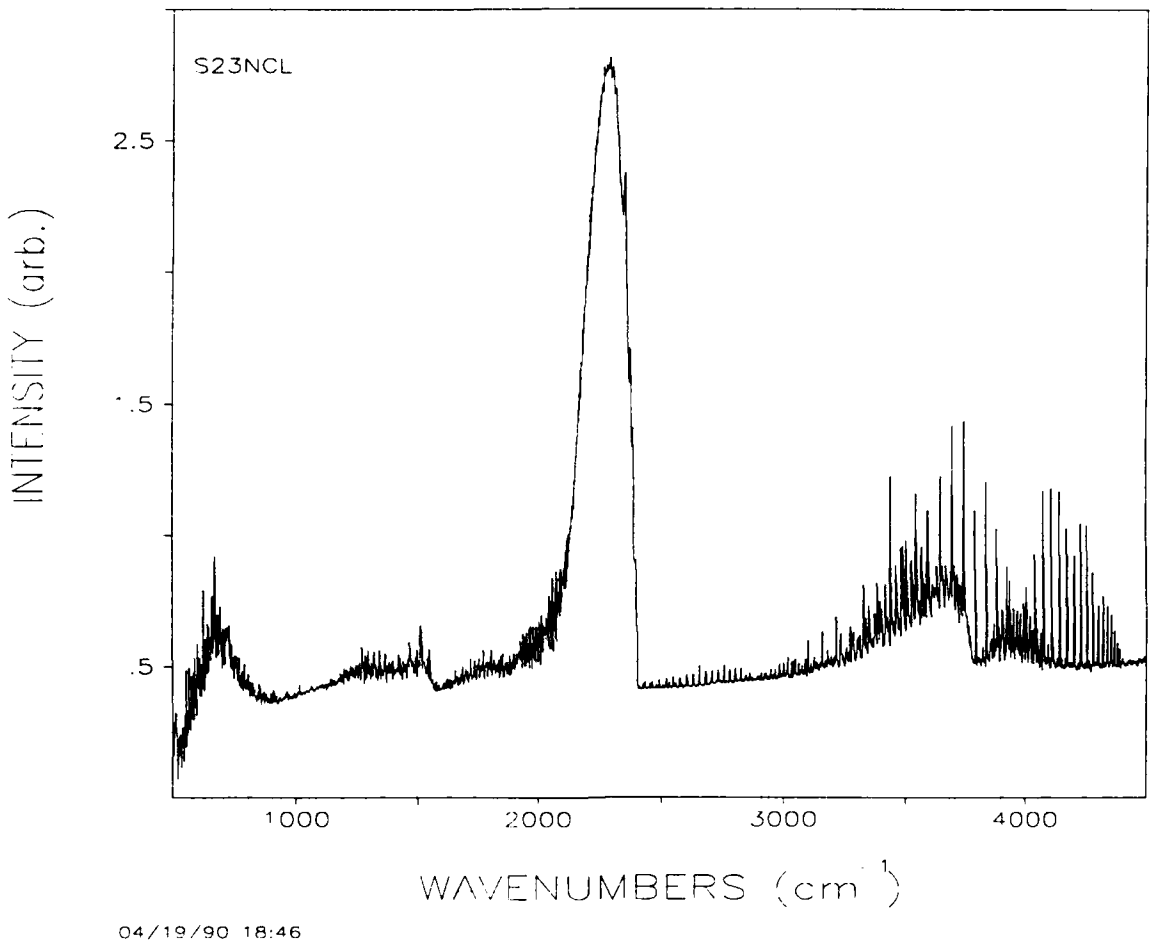

Figure 4. Penn State 4 cm^{-1} Resolution Emission Spectrum of NOSOL-363 Burning in Air.

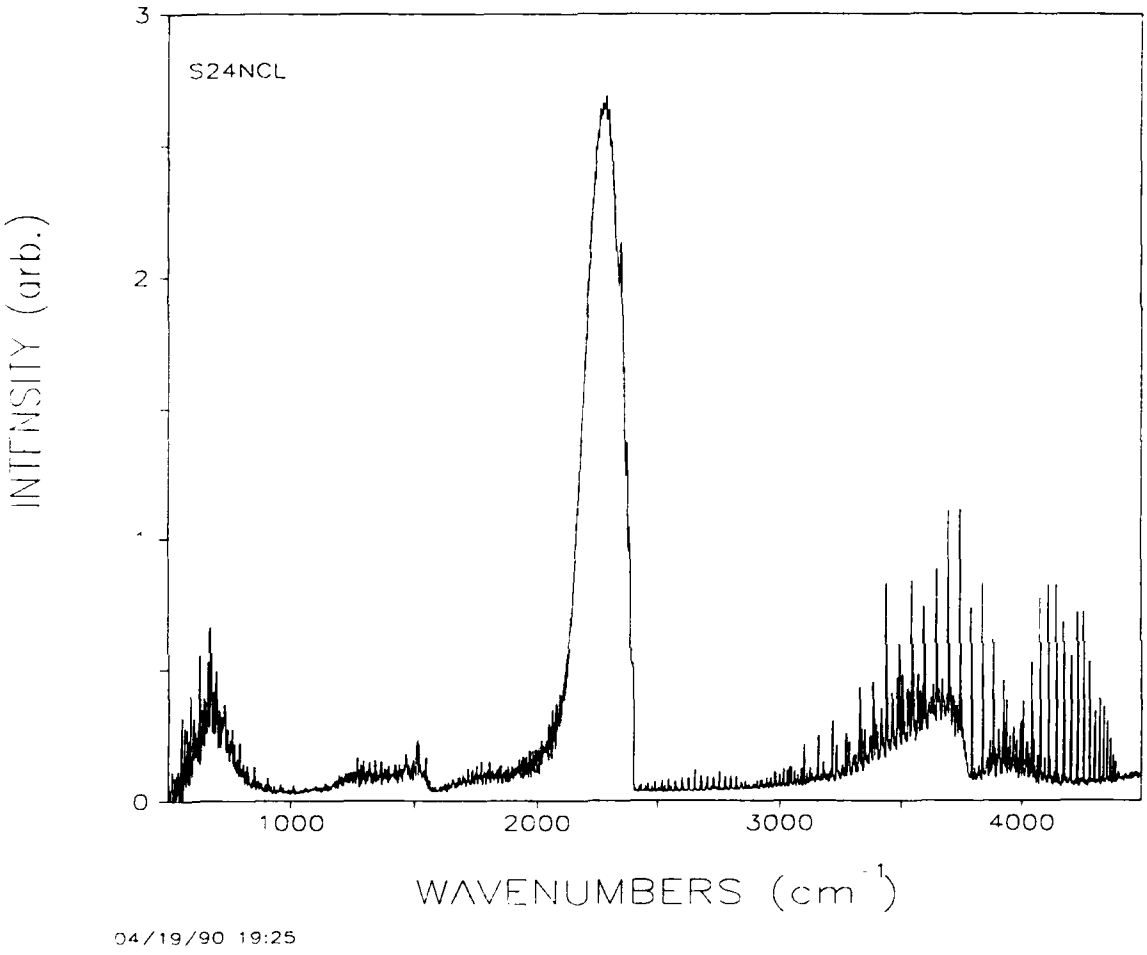

Figure 5. Penn State 4 cm^{-1} Resolution Emission Spectrum of NOSOL-363 Burning in Air. Line of Sight is 1 cm Higher than in Figure 4.

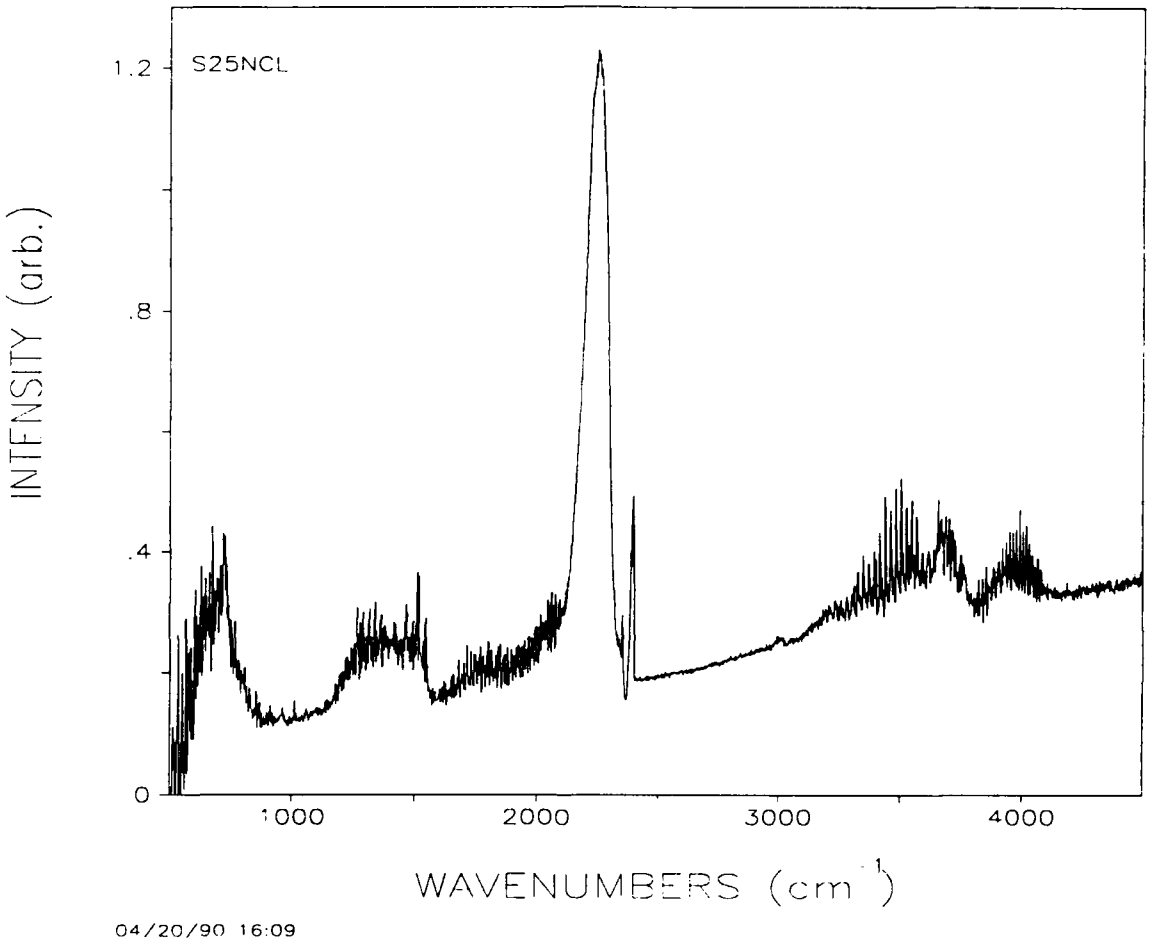

Figure 6. Penn State 4 cm^{-1} Resolution Emission Spectrum of B/BAMO/NMMO Propellant Burning in Air.

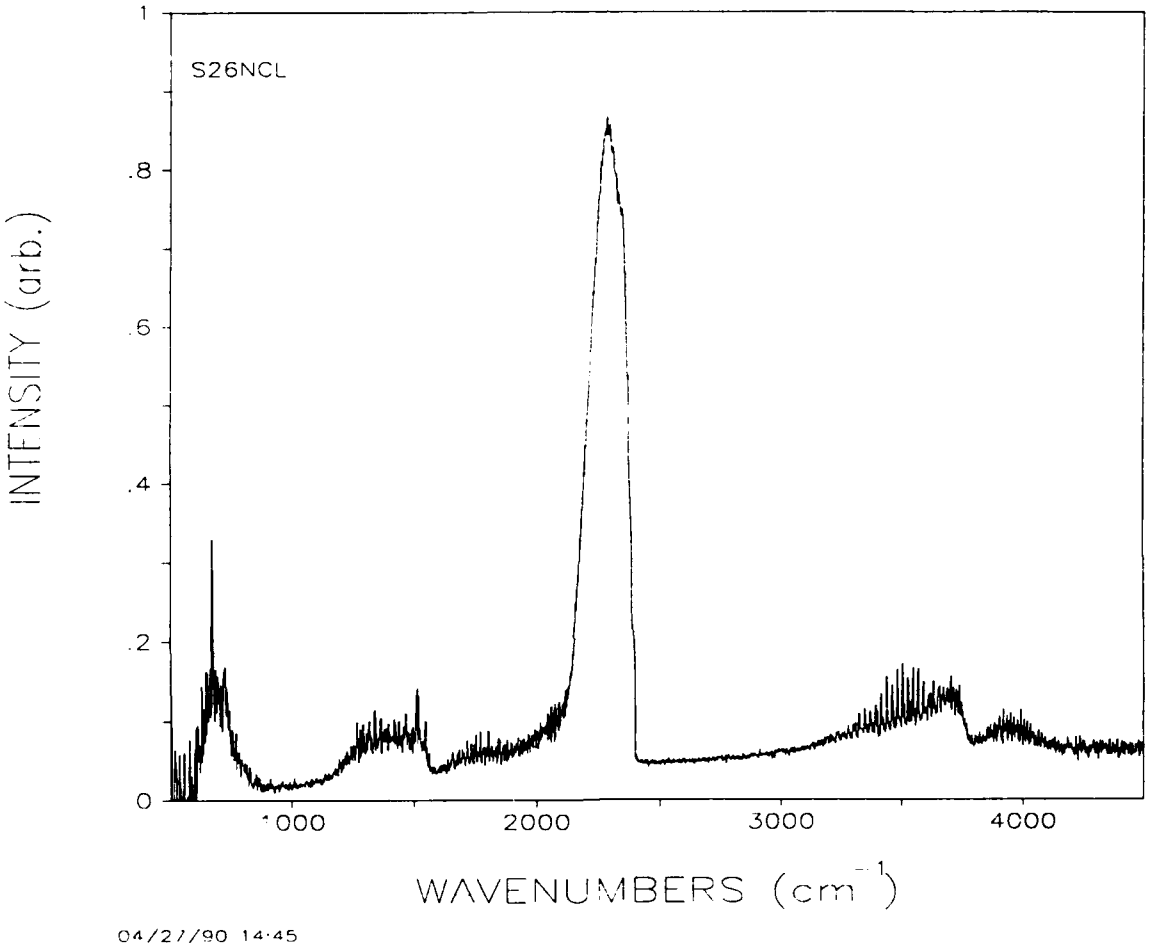

Figure 7. Penn State 4 cm^{-1} Resolution Emission Spectrum of B/BAMO/NMMO Burning in Air. Plexiglass Shields were Placed Around the Burning Strand to Minimize Recirculating Gases.

Much of the analysis work to be discussed below is done using band models of spectral radiation, in which the strengths of many spectral lines are averaged and tabulated at relatively low spectral resolutions, ranging from 5 to 25 cm^{-1}. To compare with these models, we used SpectraCalc to produce a set of smoothed, lower resolution spectra, which are displayed in Figures 8 through 13. The SpectraCalc procedure used was a 25 point Savitsky-Golay smooth. This method[1] uses a convolution approach which performs a least squares fit to the specified window of data points.

The result of this smoothing procedure on spectral features which even very roughly approximate a Gaussian shape is that the feature width and the smoothing width (the full width at half maximum equal to half of 25 times the point spacing, or about 24 cm^{-1}) add in quadrature. For an example, we take the spectral feature in spectrum S25 just below 2400 cm^{-1}. (Incidentally, this feature of the CO_2 emission band transmitted through the atmosphere is often referred to as the blue spike, as the much larger peak at still lower frequency is known as the red spike.) The full width at half maximum of this feature in Figure 6 is 16 cm^{-1}, while the smoothed feature in Figure 12 has a width of 29 cm^{-1}. However its peak height is lower, and it can be verified that the total area under the feature has been preserved. It turns out that both the Savitsky-Golay and FFT smoothing routines available in SpectraCalc do generate artifacts in the form of small ripples in what might be expected to be smooth regions of the spectra, but both seem adequate to the task of comparing band model predictions and observations.

2.1 Identification of Spectral Bands

CO_2 and H_2O Bands

In Figure 2 for the inert-atmosphere test E12 we have marked the positions of prominent bands and indicated their molecular assignments. The strong narrow feature at 670 cm^{-1} and the surrounding band in the 550 to

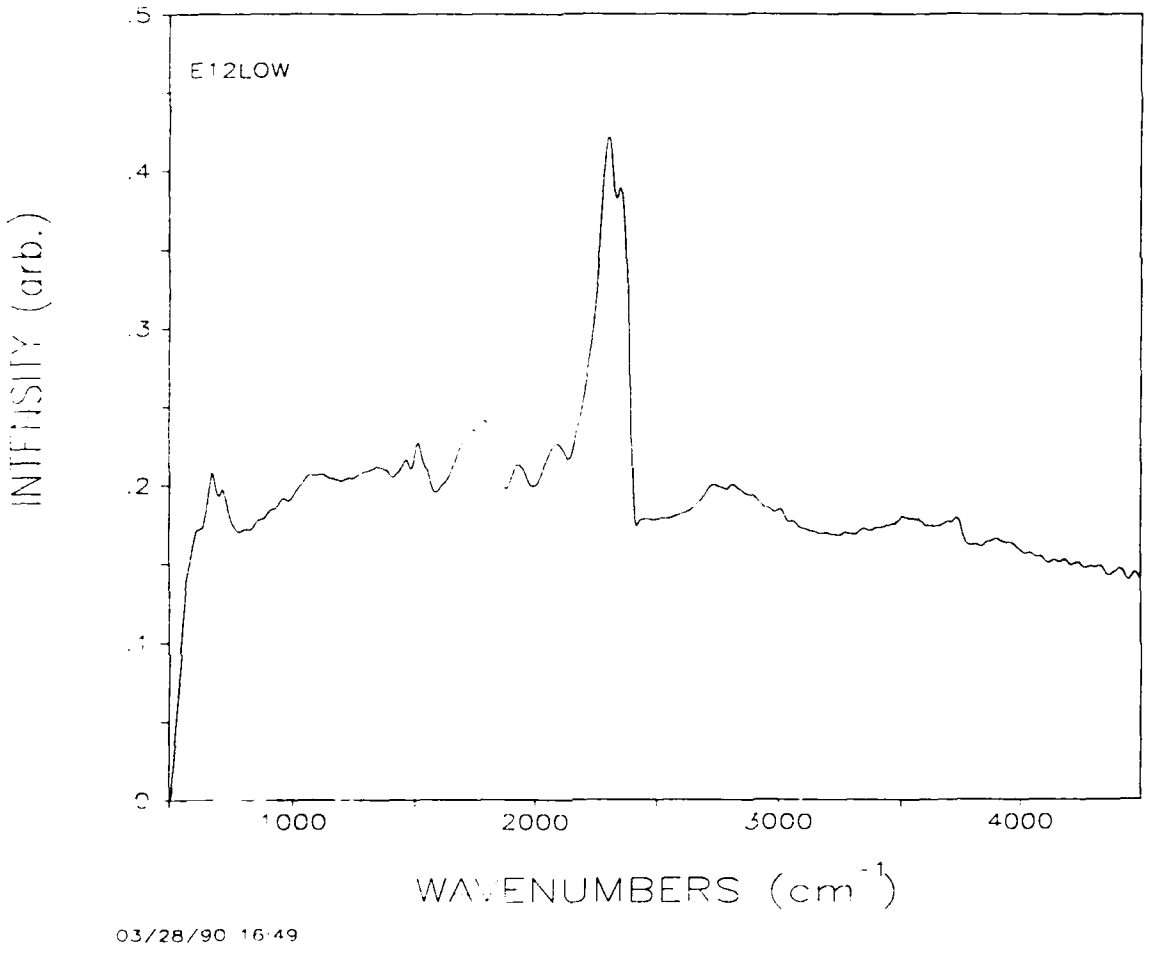

Figure 8. NOSOL-363/Nitrogen Emission Spectrum of Figure 2, Smoothed for Comparison with Band Model Radiation Predictions.

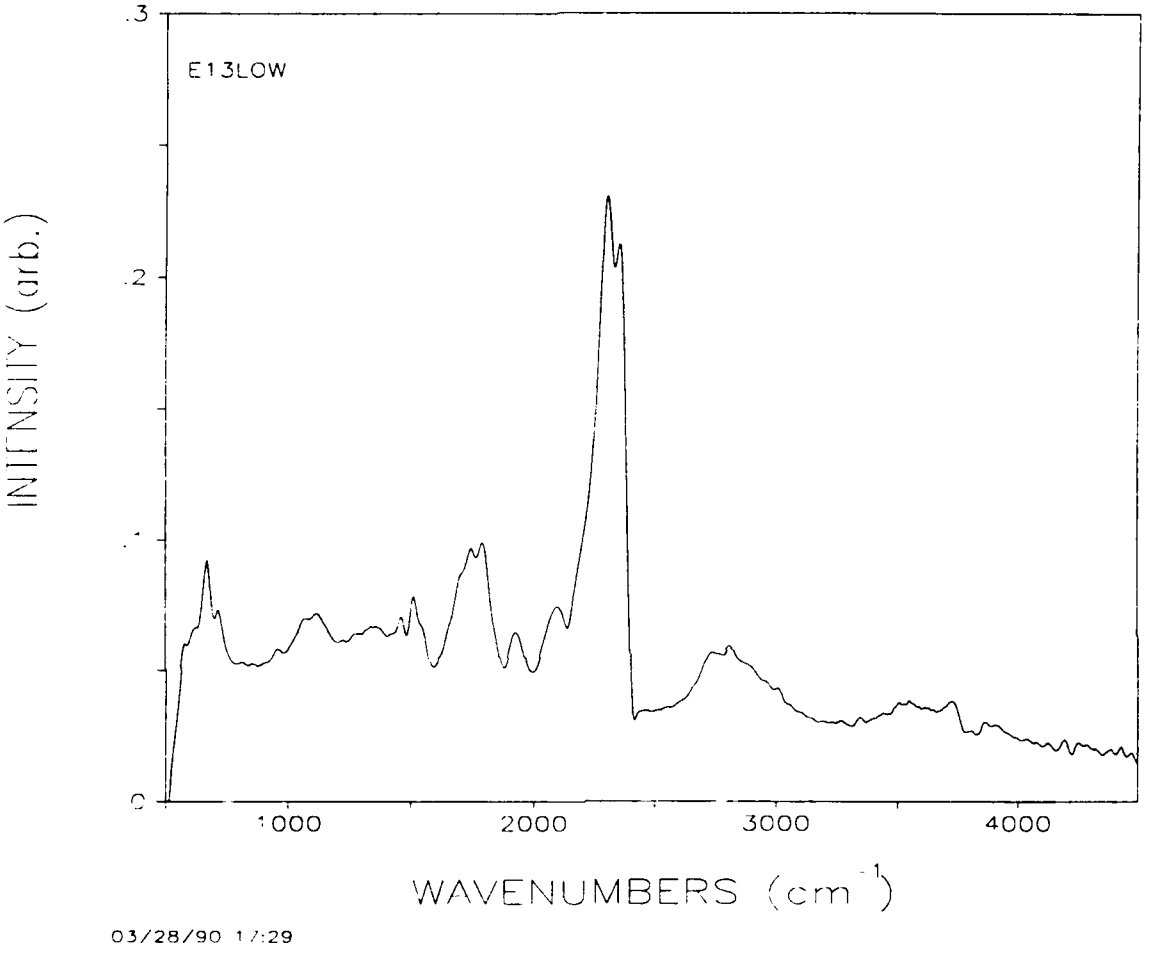

Figure 9. NOSOL-363/Nitrogen Emission Spectrum of Figure 3, Smoothed for Comparison with Band Model Radiation Predictions.

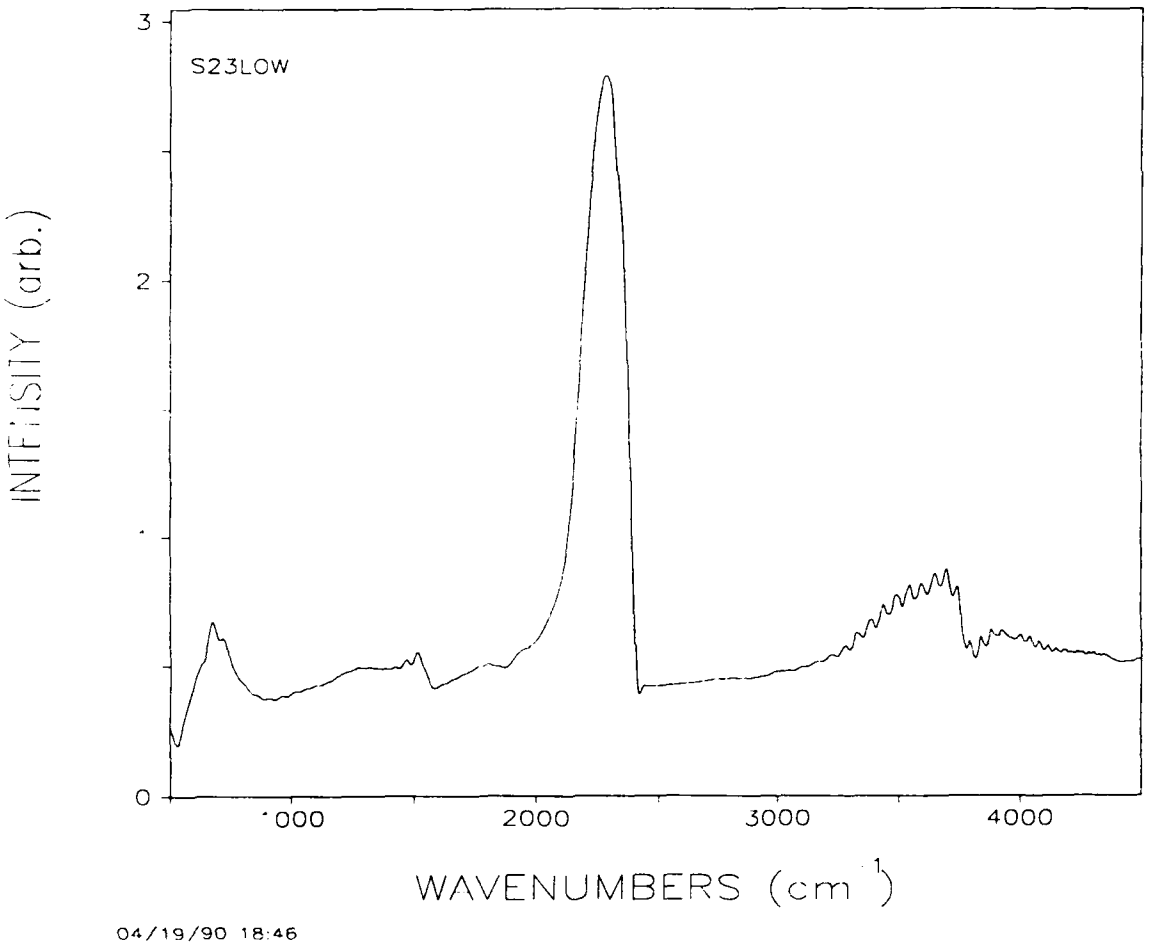

Figure 10. NOSOL-363/Air Emission Spectrum of Figure 4, Smoothed for Comparison with Band Model Radiation Predictions.

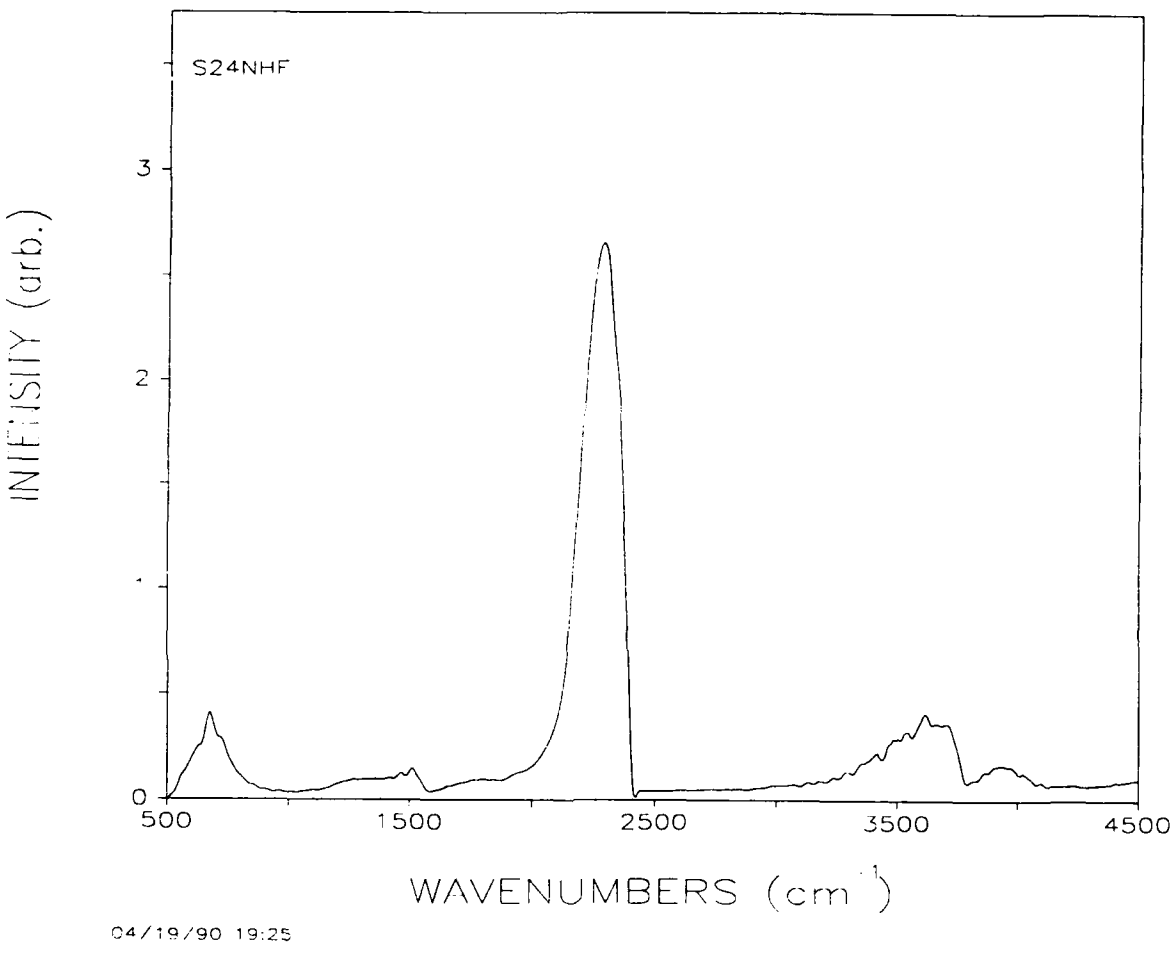

Figure 11. NOSOL-363/Air Emission Spectrum of Figure 5, Smoothed for Comparison with Band Model Radiation Predictions. (HF Emission Lines were Removed before Smoothing.)

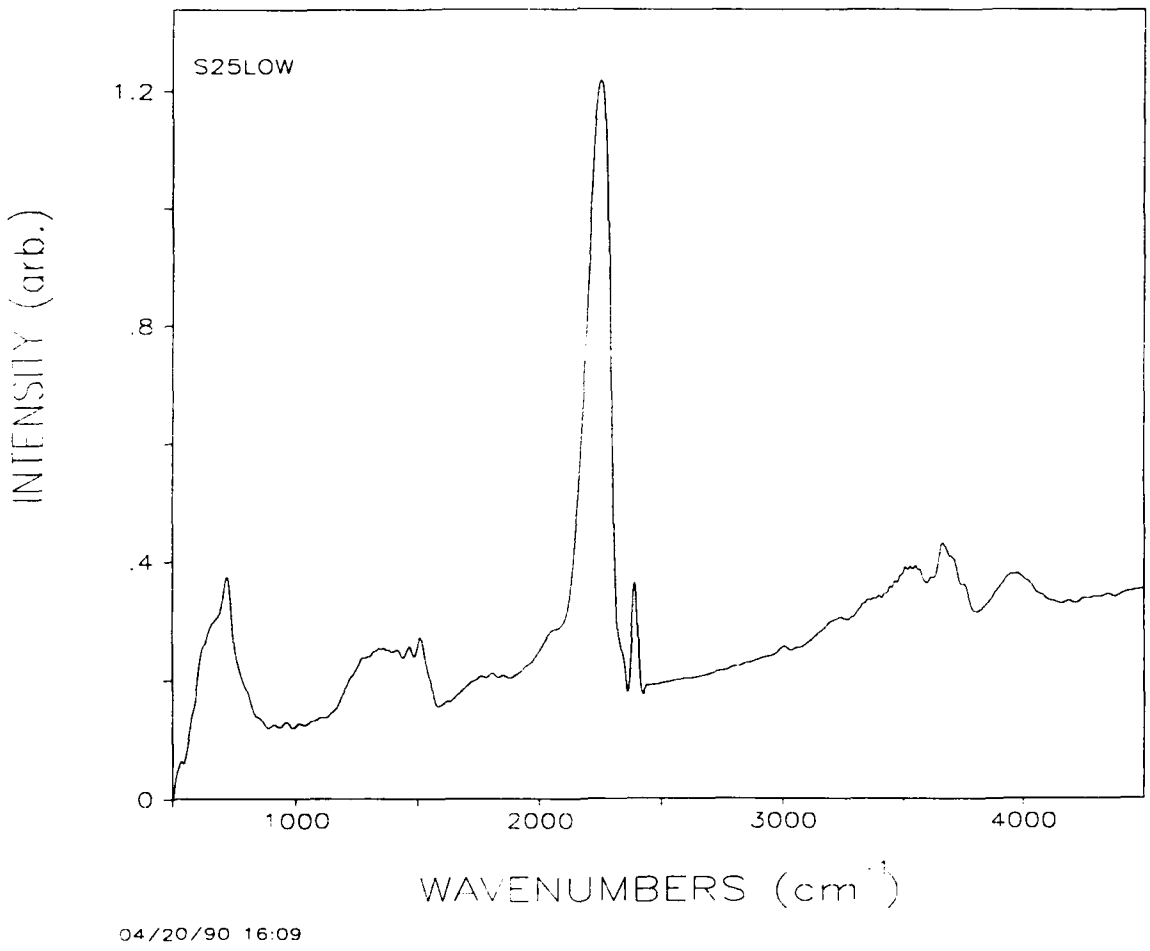

Figure 12. B/BAND/NMMO/Air Emission Spectrum of Figure 6, Smoothed for Comparison with Band Model Radiation Predictions.

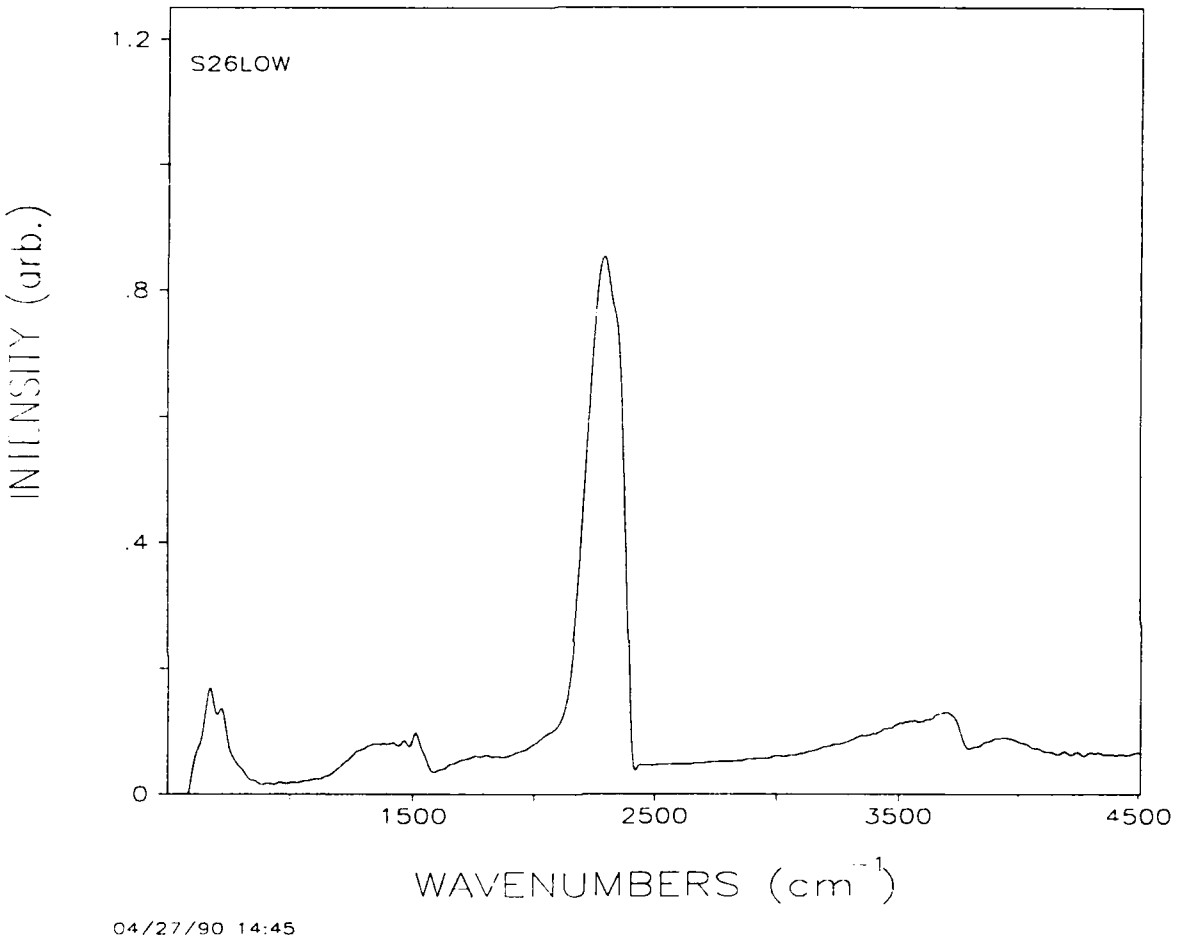

Figure 13. B/BAND/NMMO/Air Emission Spectrum of Figure 7, Smoothed for Comparison with Band Model Radiation Predictions.

800 cm^{-1} region belong to CO_2, as does the strong band from 2150 to 2400 cm^{-1}. A weaker CO_2 band also contributes to the emission in the 3300 to 4000 cm^{-1} region, but the majority of the features here are due to water. The other strong water band is clearly seen from 1200 to 1600 cm^{-1}, although a sparser distribution of water lines continues to contribute on both sides.

The CO Band

The highly structured feature in the 2000 to 2150 cm^{-1} region is due to the CO molecule. The lines of diatomic molecules are arrayed in a simple pattern of two branches extending to higher and lower frequency from the band center. The lower frequency branch, called the P branch, is composed (in absorption) of transitions in rotational quantum number J in the lower state to J-1 in the upper state, while the higher frequency or R branch is composed of transitions from J to J+1 (a Q branch of J to J transitions can appear near the band center, but only in polyatomic molecules, or in diatomic molecules with at least one state having a nonzero value of total electronic angular momentum about the internuclear axis- the sharp CO_2 feature near 670 cm^{-1} mentioned above is a Q branch). The intensity of lines of each branch follows the product of a Boltzmann distribution of lower state populations and a 2J+1 degeneracy factor.

The CO band center is at about 2143 cm^{-1}, so the contour from 2050 to 2140 cm^{-1} is the P branch, while the R branch can be seen proceeding up the side of the CO_2 band. In fact, the apparent line structure in Figure 2 is not an accurate representation of the CO band, because in the P branch the line spacing varies from 4 to 5 cm^{-1}, while the spectrometer point spacing is between 1.9 and 2 cm^{-1}. When CO line positions are close to spectrometer points, every other spectrometer point must correspond to a peak. Eventually, peak positions fall between spectrometer points and the line intensity is averaged between two spectrometer points. After this point of adjustment, the match between CO line positions and the 4 cm^{-1} resolution spectrometer point

array becomes better again, and so forth. In Figure 14, regions of good and bad match can be seen, giving the observed spectrum a pattern of constructive and destructive interference. At 1 cm^{-1} resolution, this distortion of the CO band contour would not occur.

The H_2CO Bands and the NO Band

The sharp peak just above 1750 cm^{-1} is the Q-branch feature of the H_2CO (formaldehyde) ν_2 band. At least 4 other spikes can be seen in the 1750 to 1800 cm^{-1} region, some or all of which may be Q-branches of hot bands of H_2CO (transitions originating in excited vibrational states, beginning with the 2-1 transition). Although this band is in the region of strong isolated water lines, comparison with spectra of hydrocarbon flames in air shows no match with any of these peaks. The band just to higher frequency from this H_2CO band, peaking at 1930 cm^{-1}, is in fact the R branch of NO, whose P branch is hidden under the H_2CO band.

The less structured contour of emission stretching from 2600 to 3100 cm^{-1} is also due to H_2CO, and is in fact two overlapping bands, the ν_2 band centered at 2782 cm^{-1} and the ν_5 band centered at 2843 cm^{-1}. While low pressure spectra of this region show a number of clearly resolved Q-branch features, the flame spectra are relatively smooth. This could be due to more energy levels being populated at higher temperatures, or it could be due to overlap with a band of a second molecule. The latter seems unlikely, since the strength of the ν_1/ν_5 band region is about twice the ν_2 band strength, seemingly leaving little room for an additional contribution in the 2600-3100 cm^{-1} region if the literature ratio is to be maintained.

An Unidentified Band in the Inert-Gas Spectra

The E13 spectrum in Figure 3 has all the same features as the E12 spectrum in Figure 2. In addition, the lower continuum intensity makes it

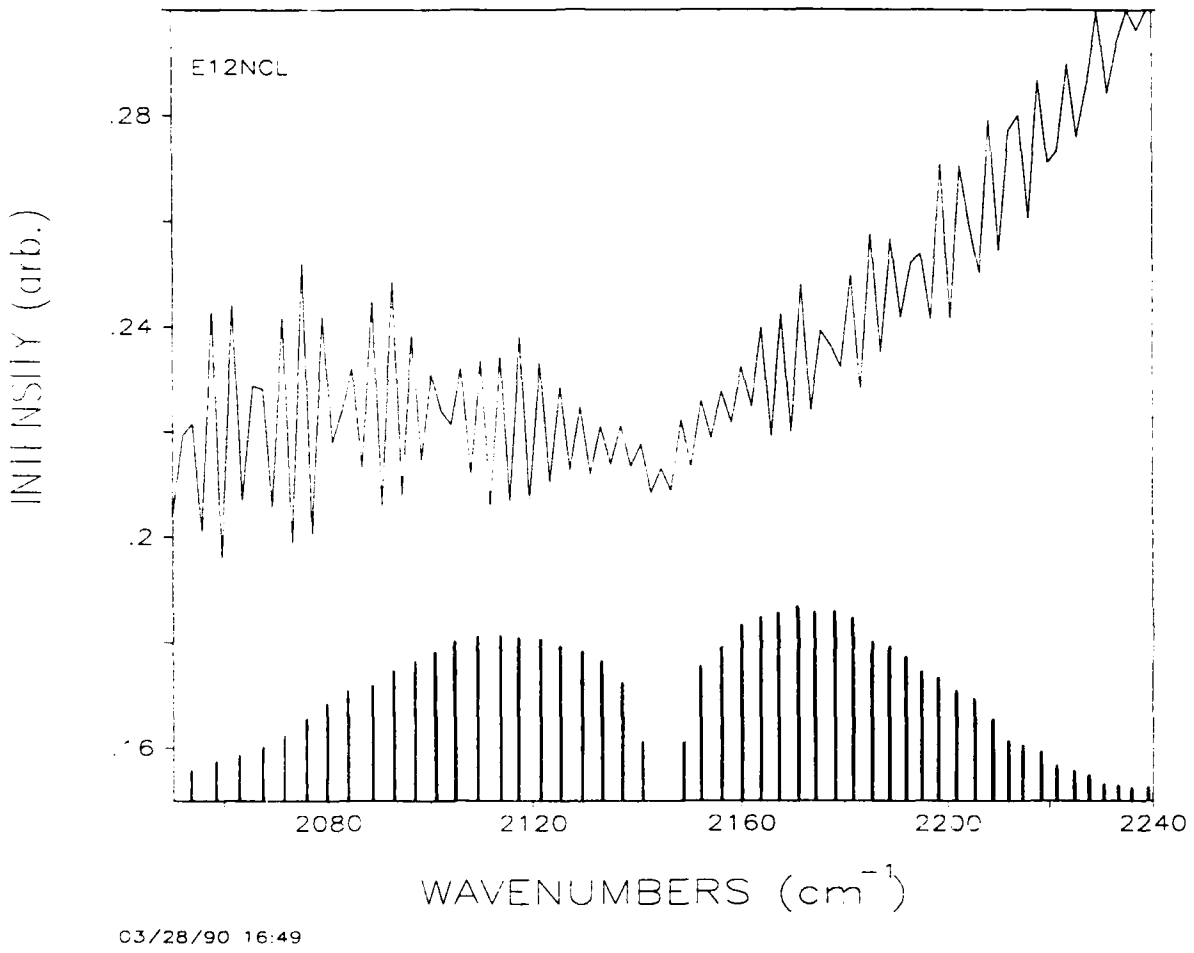

Figure 14. Expanded View of CO Emission Region of Figure 2 (top), Compared with Room Temperature CO Band Profile (bottom).

easier to see that there is an additional molecular emission band in the 930 to 1200 cm^{-1} region, composed of a broad, featureless peak centered at 1100 cm^{-1}, and (perhaps) a much smaller and narrower peak at 950 cm^{-1}. In this section we discuss various possible assignments for this band.

We begin by noting that it does not appear in the combustion-in-air runs of the last four spectra. (In fact, except for the HCl and HF bands in S23 and S24 to be discussed below, the only molecular species observed in the air combustion spectra are H_2O, CO_2, and CO.) Thus we can assume that it is a species which would be consumed in the higher oxygen, higher temperature environment of air combustion.

Another general comment which can be made is that the lack of spectral structure in the unknown band indicates that it is heavy enough that the spacing between rotational lines is smaller than the spectrometer resolution (unlike CO, for instance) or that it is a complex enough molecule that many lines combine to make a pseudo-continuum (like H_2CO in the 2600-3100 cm^{-1} region). On the other hand, the fact that only one band is observed can mean one of three things: the radiator is a diatomic molecule (unlikely since no P-R structure is seen); it is a polyatomic molecule with only one strong absorption band (there are few of these); or, it has several strong bands, but the others are hidden under bands already assigned to other molecules.

An examination of the spectra of gas phase products of pyrolysis of RDX taken by Oyumi and Brill[2] shows no evidence of an absorption peak at at 1100 cm^{-1}. This does not necessarily mean that the unknown molecule must contain another element beyond the carbon, nitrogen, hydrogen and oxygen which make up RDX- it may simply be that the initial bond-breaking steps in the two propellants are different enough that their primary decomposition products are different.

Because the NOSOL propellant contains potassium sulfate as an after-burning modifier, it was natural to consider sulfur species as candidates. However, the species with the closest spectral match, SO_2, can still be ruled out as follows. The SO_2 ν_1 band does indeed have its center at 1150 cm^{-1} and, at room temperature, does extend to about 1100 cm^{-1}. Changes in band shape at higher temperatures might make it impossible to dismiss without more detailed analysis, if it were not for the presence of an 8 times stronger band[3] peaking at just above 1360 cm^{-1}, a feature which is not observed in the Penn State spectra.

A similar argument can be made against HCO, whose matrix isolation spectra[4] show a strong peak around 1090 cm^{-1} assigned to the ν_2 or bending vibration and subsequently seen in several gas phase observations[5]. However, the ν_2 band centered at 2435 cm^{-1}, though weaker, should also be visible, yet there is no hint of any emission feature in the 2400-2600 cm^{-1} region.

In searching the literature for stable molecules with bands which might match our unknown, a valuable starting point is the tabulation of Shimanouchi.[6] We should mention that one of the most common reference books for infrared spectra of organic compounds, the Aldrich Library,[7] contain only spectra of liquids. This is presumably the reason that its spectrum of formaldehyde includes a very strong, broad absorption band centered at 1100 cm^{-1}, while the gas phase spectra[8] have no such feature. We also searched two very useful references,[9,10] which do present gas phase spectra.

Among stable molecules, the best match between a reported band position and the unknown is acetaldehyde (CH_3CHO), which has a strong band centered around 1110 cm^{-1}, as well as a similarly strong band around 2750 cm^{-1} and an almost ten times stronger band around 1750 cm^{-1}. Both of these latter bands could perhaps be part of features already assigned to formaldehyde. However, acetaldehyde also has a band in the 1300-1500 cm^{-1} range with several strong Q-branch features which are not observed in the Penn State spectra, so at this point this looks unlikely.

By comparison, the spectrum of methanol is relatively simple, with the strongest band extending from 960 to 1090 cm^{-1} at room temperature, and having weaker bands in the 2800-3100 and 1200-1500 cm^{-1} regions which could be hidden in the H_2CO and H_2O bands respectively. Here, the serious problem is not in extra bands which are not observed, but in the bad match between the shape of the strongest band and the unknown feature. The methanol band has a prominent Q-branch feature near its band center around 1035 cm^{-1}. Detailed modeling might show otherwise, but a priori it seems unlikely that a higher temperature band shape would completely lack this Q-branch and would have its peak shifted all the way from 1035 to 1100 cm^{-1}.

Therefore, although these last molecules are certainly plausible decomposition products to find in a system which clearly produces copious H_2CO, we are unable to find any completely convincing match. More in-depth work in constructing high temperature band models of some of the candidates, or in using band model predictions to remove some features from the observed spectrum in order to find whether unobserved bands lie beneath them, might still result in an identification.

Molecules Sought and Not Found

It seems worthwhile to report here work done in examining spectra for evidence of emission from a few molecules with strong, well characterized bands, in which the conclusion was that the emission, if any, did not exceed the noise level.

The strongest NO_2 band around 1620 cm^{-1} has a dense spectral structure even at room temperature, as can be seen from the 2 cm^{-1} resolution spectrum of Reference 11. At higher temperatures, much of this structure would be further reduced towards a pseudo-continuum spectrum. We compared peak positions in the Reference 11 spectra with peak positions in the Penn State spectra and found no match, concluding that emission from NO_2 is not

observable against interfering spectral features and noise in the Penn State spectra taken to date.

Propellant combustion mechanisms of the chemistry of the NO_2 group include its conversion into HONO, and NO (which may also be formed from HONO), as well as reactions of NO to form HNO or N_2O (N_2O may also be a direct propellant decomposition product). HONO has two bands with prominent Q branches around 785 and 850 cm^{-1}. With the noise level and resolution of Figure 2, these features are not visible. HNO has a band[5] at 1570 cm^{-1} which is, again, not observed. Similarly, no evidence can be seen in Figure 14 for the strong N_2O band centered at 2224 cm^{-1}, and the weaker band in the 1250-1300 cm^{-1} region also gives no apparent contribution.

The strongest absorption features of the ammonia molecule are at 930 cm^{-1} and a little above 960 cm^{-1}. These features are not convincingly seen in Penn State spectra. Finally, a series of possible spectral regions for emission from boron-containing molecules was examined in the S25 and S26 spectra. No emission was seen, in agreement with our expectation that the boron particles do not burn under the conditions of those observations.

2.2 Temperatures from Rotational Line Intensities

As mentioned above, the intensity of individual vibrational-rotational lines is related to a Boltzmann distribution of the populations of the lower states, so that line intensities can be used to deduce a temperature which should be in equilibrium with the translational or gas kinetic temperature. In principal the ratio of any two lines gives a temperature, but for greater precision a least squares fit to as many lines as can be observed is desirable. The details of this analysis are discussed in Reference 12. Here we will simply present the formula we used with a few explanatory comments.

A key point to be made is that, following the discussion in Reference 12 of relating peak absorbances observed with a spectrometer of finite resolution to the true peak absorbance or optical depth, the observed line peak heights in the Penn State spectra can be related to a true emissivity which would be observed by a spectrometer having infinite resolution, and which in turn can be related to the concentration that particular rotational state of the emitting molecule. For lines which are optically thin, an increase in concentration is reflected by a linear increase in both the true peak height and the peak height of the finite resolution line. However, for lines which are optically thick, the true peak height does not change, though the wings do rise in intensity, causing lines to broaden when the molecular concentration (or path length) is increased.

It turns out[12] that when the area under these wider lines is (in effect) integrated by a spectrometer resolution function, the apparent peak absorbance observed in finite resolution increases as only the square root of the true absorbance or optical depth. Although the emissivity (ε), the quantity observed in emission spectra, is related to the absorbance A by

$$\varepsilon = (1-e^{-A})$$

we still expect that an observed finite resolution emissivity or line peak height will increase more slowly than the true optical depth which is proportional to molecular concentration, and that this rate of increase will also be approximately as the square root of the true optical depth. Therefore, we will use a formula which relates the square of N, the observed emission line peak height, to an expression for the dependence of the true optical depth on temperature. When this formula is rearranged into an equation which can be plotted to estimate the temperature, we obtain

$$-\ln(N^2(m)\gamma/N^\circ |m| F(m)\nu^4) = E(m)/kT + C \qquad (1)$$

In other words, a plot of the quantity on the left versus lower state energy E will have a slope of 1/kT, where k is the Boltzmann constant in cm^{-1}/K. Also in this expression, N° is the blackbody intensity at the emission temperature, ν is the line frequency in cm^{-1}, m is the line index (J+1 in the R branch, -J in the P branch), F(m) is the Herman-Wallis factor which describes the change in transition probability with increasing rotational energy, and γ is the true, pressure-broadened width of the line. This linewidth is in general a function of the line index as well, but a model we developed based on existing measurements indicated that at the temperatures important here, it might be close enough to constant that this dependence could be ignored.

It should be noted that, because of the logarithm in Equation 1, a change in a multiplicative constant in the quantity in parentheses simply changes the value of the constant C, without affecting the slope and therefore the temperature determination. Because of this, the fact that both the linewidth and the blackbody function depend on temperature does not in fact require an iterative procedure. The blackbody function, whatever temperature is chosen at which to evaluate it, is simply a multiplicative constant with no dependence on line index. The temperature dependence of the linewidth is in principal a function of line index, but in practice, as stated above, we make the assumption that throughout the temperature range of interest the linewidth is independent of line index, so that choosing a nominal value for the linewidth is sufficient.

We applied Equation 1 to the HF and HCl lines observed in the S24 spectrum exhibited in Figure 5. The HF and HCl did not come from propellant ingredients, but rather from halocarbon grease applied to the side of the propellant strand to discourage burning down the side. Expanded views of the two spectral regions of interest are given in Figures 15 and 16.

Figure 17 gives a plot of the quantities in Equation 1 for the HF band. We report a temperature of 1900 ± 100 K, based on the fact that a least squares fit through only the black points gives a temperature of 1825 K, while

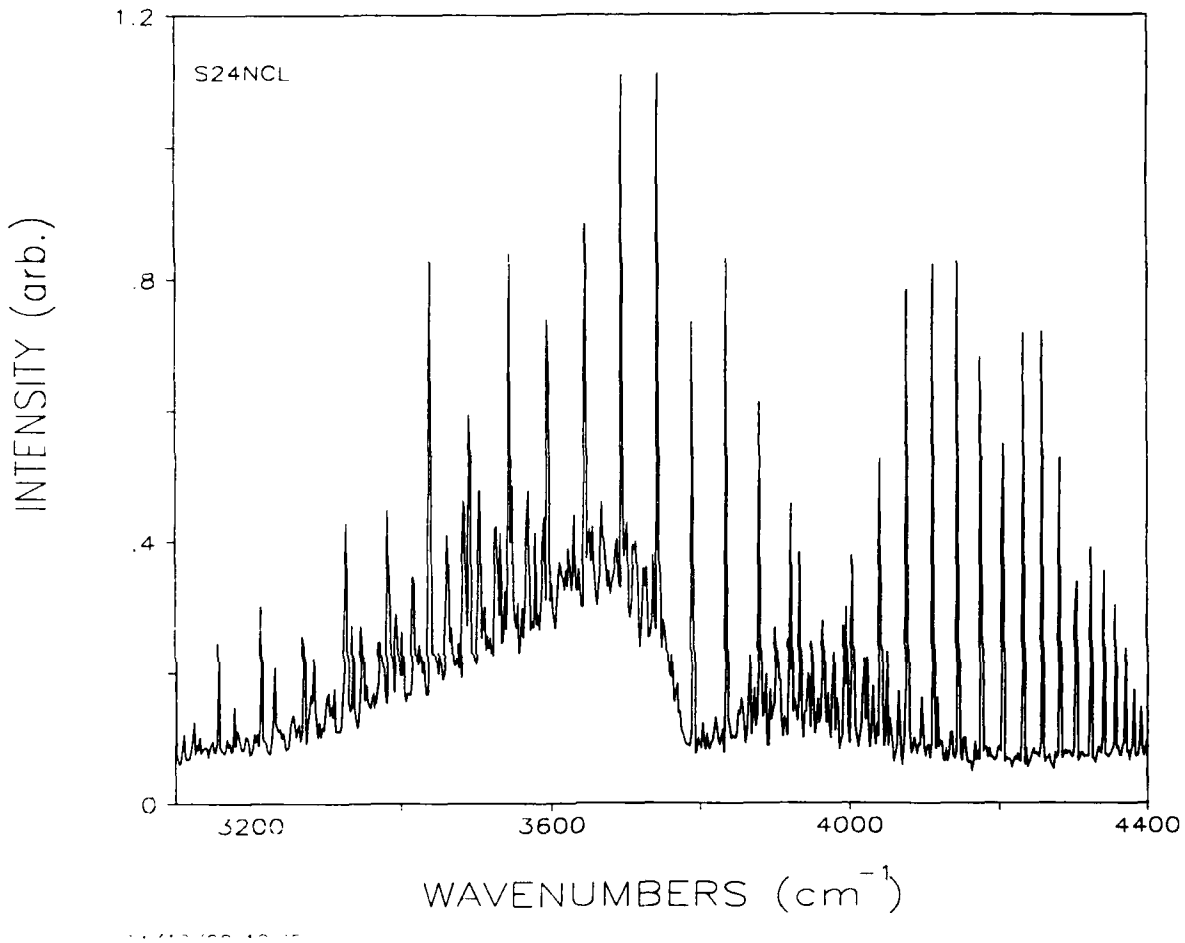

Figure 15. Expanded View of HF Emission Region of Figure 5.

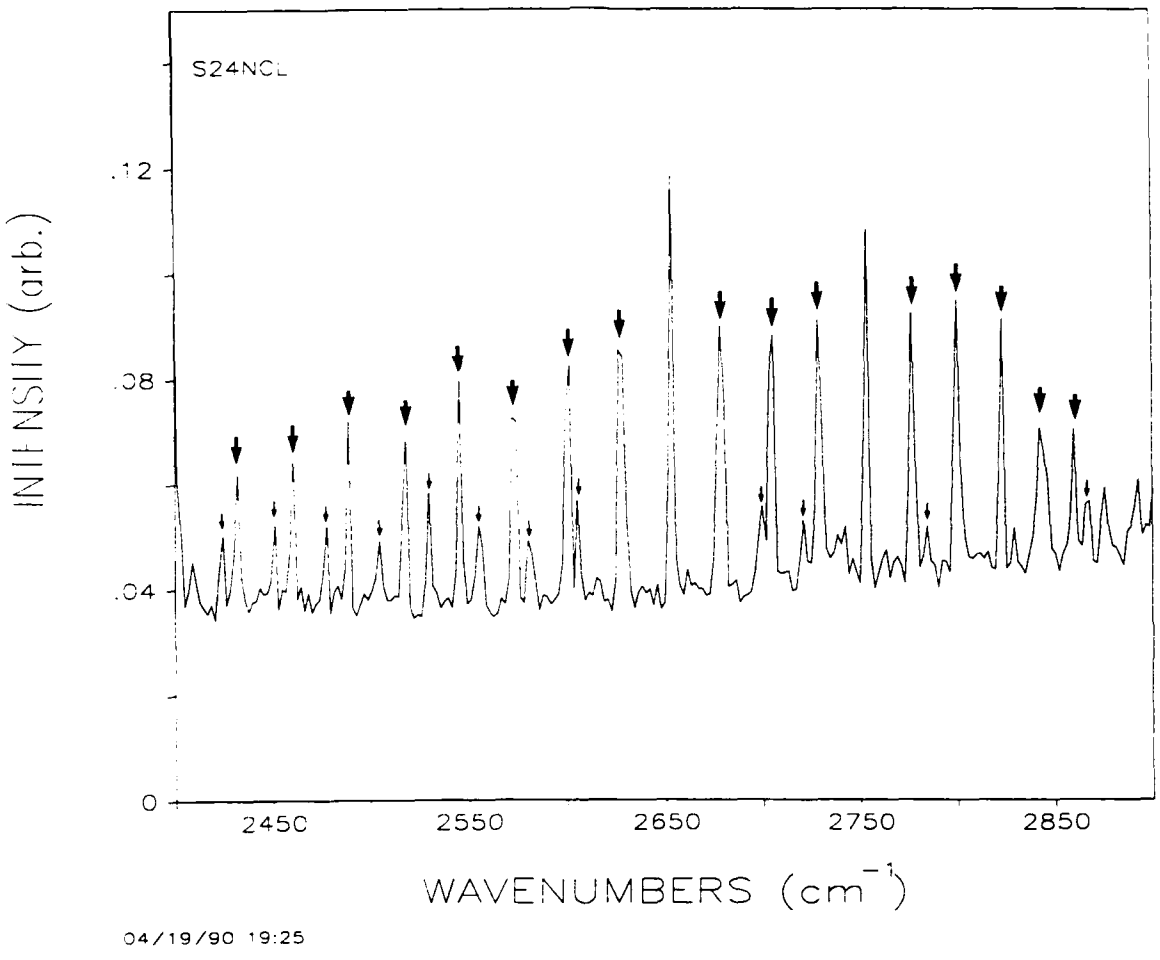

Figure 16. Expanded View of HCl Emission Region in Figure 5. Large Arrows Denote 1-0 Band Lines Used in the Temperature Plot of Figure 18, and Small Arrows Indicate 2-0 Band Lines Used in Figure 19.

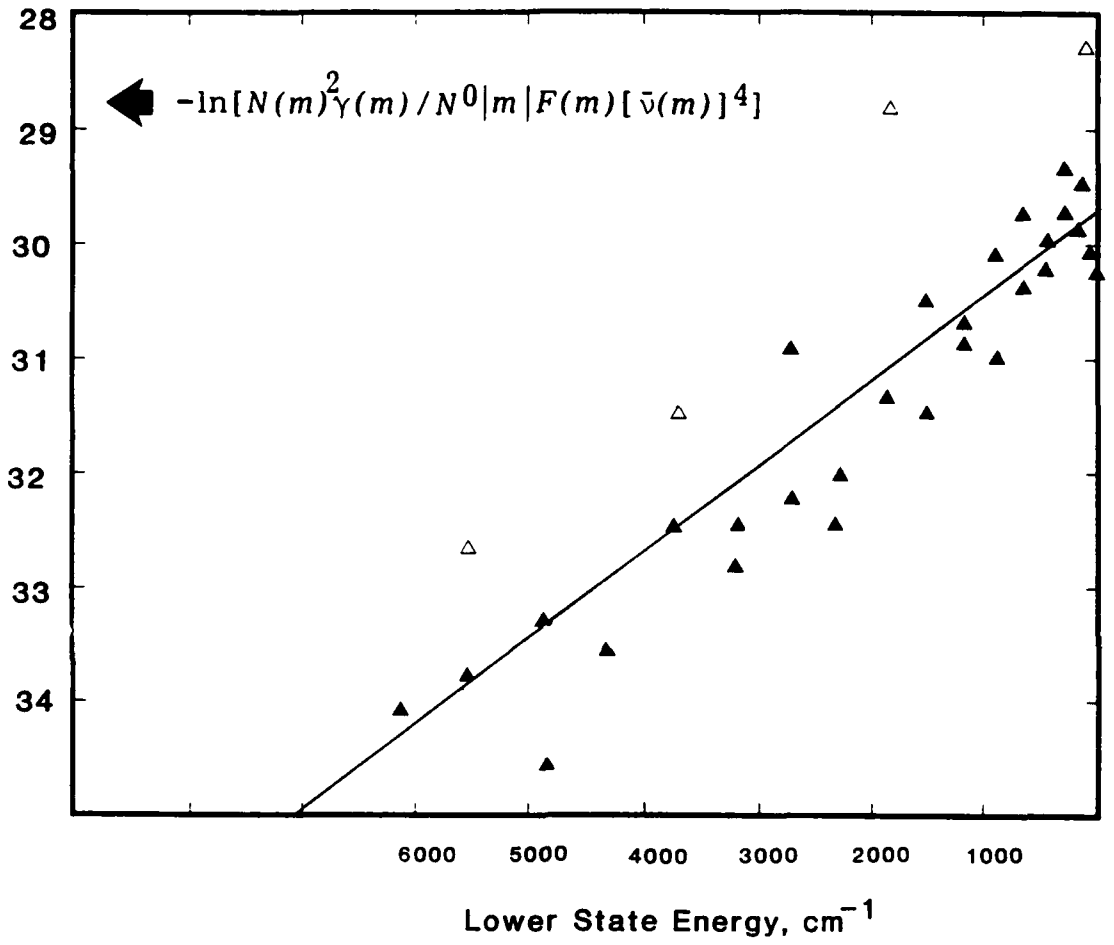

Figure 17. Temperature Plot Using Observed HF Line Peak Intensities from Figure 15 as N(m). Slope of Indicated Least Squares Line, Fit to All Points, Gives a Temperature of 1900 K. A Fit Ignoring Four Open Points Yields 1825 K.

including the white points gives 1900 K. It should be said that in this example and the HCl examples to follow, the choice of points to drop or include as possible outliers was made on the basis of their appearance in the spectrum, before the plot was made, and not on how close they were to the fitted line.

Figure 18 is the same plot for the lines of the HCl 1-0 band, those marked with heavy arrows in Figure 16. A fit through the black points gives a temperature of 2082 K, which changes to 2022 K when the two points marked with arrows are ignored, and to 2240 K when the three white points are included.

Finally, Figure 19 is a third plot, based on the HCl 2-1 (hot band) transitions indicated in Figure 16 with light arrows. Here, the slope gives a temperature of 2165 K. Note that in this figure the quantity plotted on the ordinate only includes a single power of N(m), because these much weaker lines have been assumed to be optically thin.

The fact that all derived temperatures are very close gives us confidence in this method. Some of the scatter in individual points could be reduced if integrals instead of peak heights were used, and more could be removed if a higher spectrometer resolution were used. The method is especially attractive because it does not rely on fluorine or chlorine contained in the propellant. Of course, many propellants do contain at least some of one element or the other, but the procedure of coating the strand with halocarbon grease seems to raise it to the level of a general technique. Perhaps the best check of its general validity would be a set of grease/no-grease spectra with fully resolved CO emission, to show whether applying the grease changed the combustion temperature.

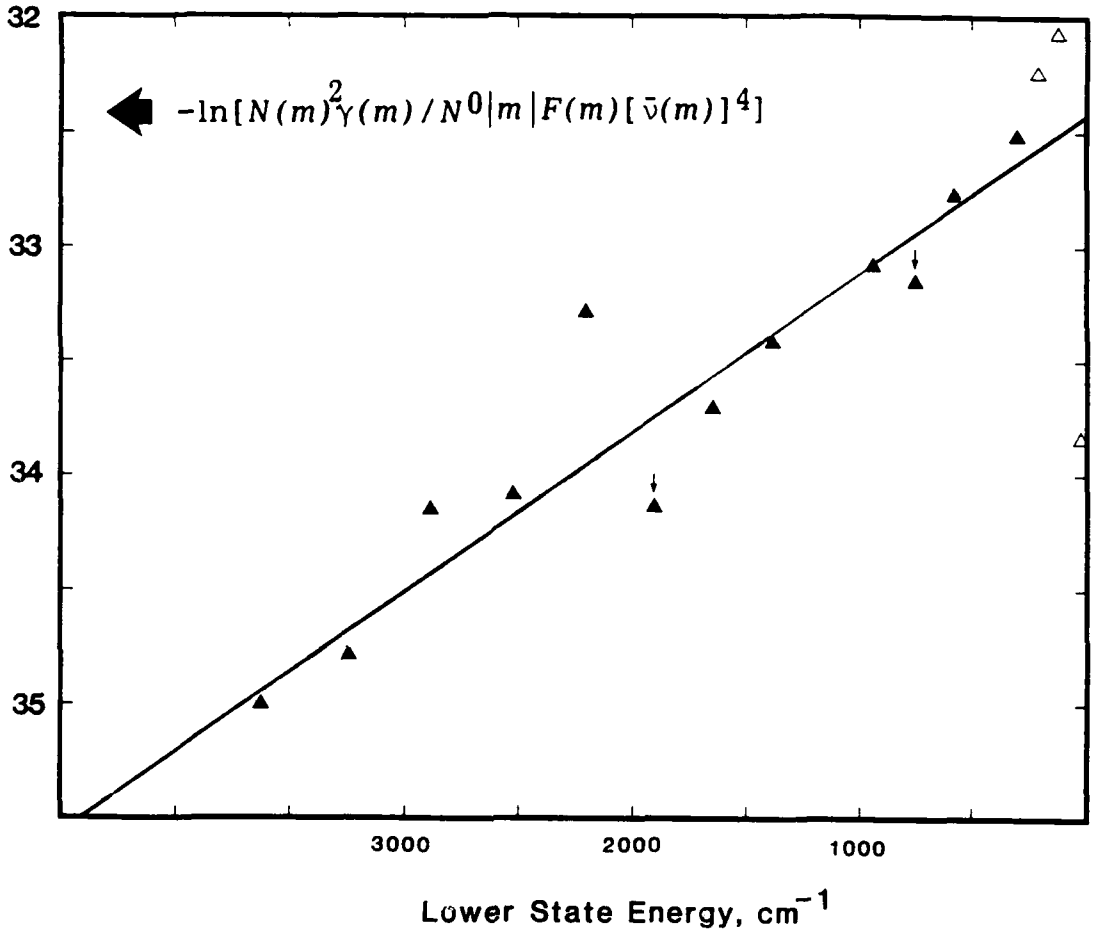

Figure 18. Temperature Plot Using Observed 1-0 HCl Line Peak Intensities from Figure 16 as N(m). Slope of Indicated Least Squares Line, Fit to All Black Points, Gives a Temperature of 2082 K. Excluding the Two Points Marked with Arrows Gives 2092 K, While Including the Three Open Points Gives 2240 K.

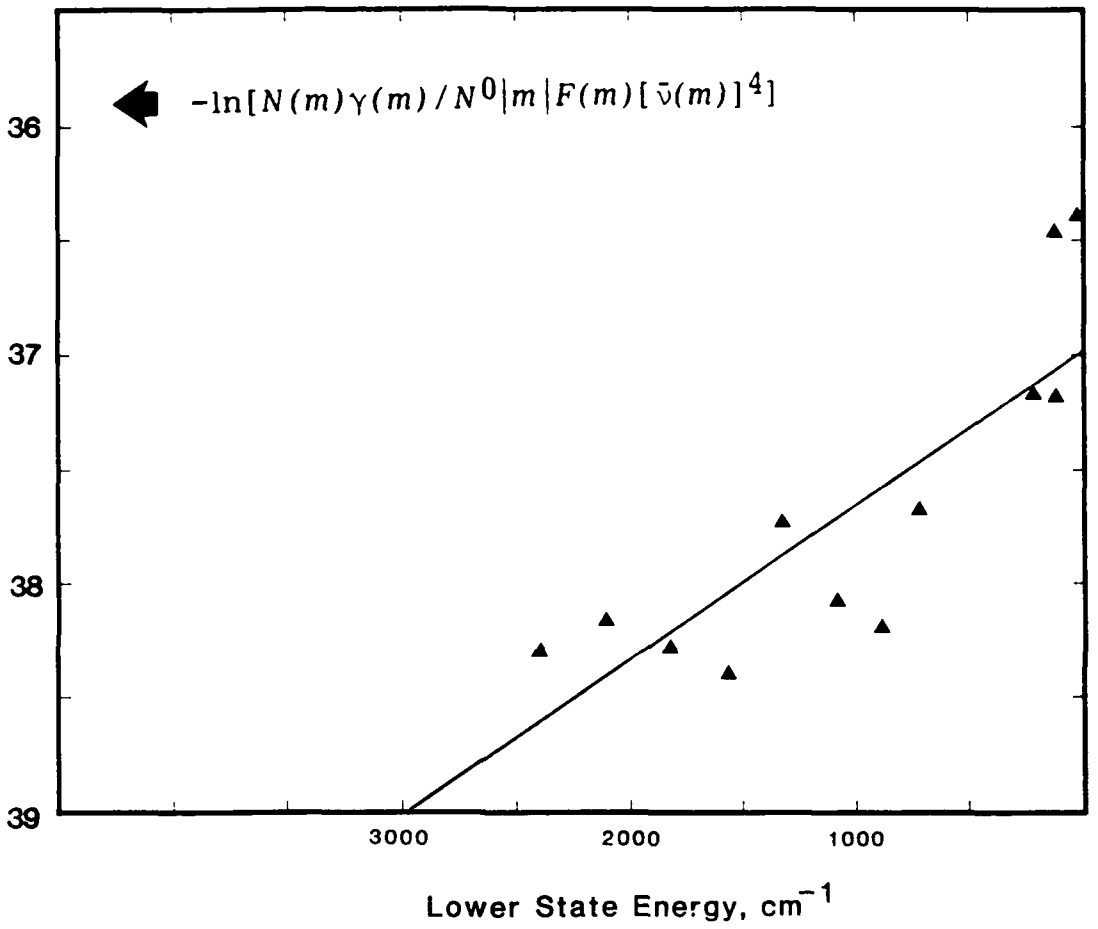

Figure 19. Temperature Plot Using Observed 2-1 HCl Line Peak Intensities from Figure 16 as N(m). Slope of Least Squares Line Gives a Temperature of 2165 K.

3. DETAILED MODELING OF OBSERVED SPECTRA

3.1 Strand Burner Fluid Dynamic Modeling

During the first part of the contract while we were waiting for observations to begin at Penn State, we wanted to assess the adequacy of existing computer codes to predict the strand burner flame flowfield. Because, as mentioned above, the strand burner is operated with purge gas flowing parallel to the axis of the strand, the flowfield resembles coflowing jets, with the primary jet being the combustion products evolving from the burning surface and the secondary jet being the low velocity, coflowing purge gas.

The one immediately available computer code which can handle this problem is the BOAT module of the Standard Plume Flowfield (SPF) code.[13] This module is an axisymmetric jet mixing model which includes finite rate chemistry. Both the Prandtl mixing length and k-ε2 turbulence models were investigated in a first cut model of the strand burner flowfield. We have used this code to model a wide variety of flames beyond the aircraft and rocket afterburning plumes for which it was originally designed. We have found it to be useful, especially when the goal is simply to compare between flames, but have also encountered several drawbacks, two of which played significant roles in limiting its usefulness in the work reported here.

First, we ran turbulent mixing calculations of nonreacting coflowing jets with velocities and pressures in the range of typical strand burner conditions. Using both turbulent mixing models, we calculated relatively long, thin flowfields. We made comparisons against what little data and analytical models we could find treating similar coflowing jets, and concluded that BOAT mixing was relatively slow. When video recordings of Penn State burns became available, we verified what we had expected from previous experience- the BOAT flowfields are much differently shaped than the observed strand burner flames, which are at times almost spherical.

We have found from our rocket plume analysis that these differences in shape do not necessarily mean that the predicted species mole fractions and temperatures will not be reasonable. On the other hand, the wrong shape can sometimes be a problem in predicting the proper appearance of optically thick regions of the spectrum One can imagine combining video observations and BOAT predictions into a semi-empirical flowfield for input to the ARC radiation calculation, which would lead to greater understanding than either source alone.

A second problem which is more difficult to get around also surfaced in our first efforts to predict strand burner flowfields using BOAT. Once a reasonable set of chemical reactions was added to the flowfield calculation (reactions already used in the one-dimensional chemical kinetics calculations discussed in the following subsection) it encountered fatal numerical problems and could not be completed. The equations involved in chemical kinetics calculations are renowned for the property of stiffness, meaning that large changes in some variables are encountered over very short time scales, while other variables only change over long time scales. With more work than we wanted to invest at this point in the program, it may well be possible to modify BOAT to take advantage of numerical techniques developed in other chemical kinetics programs especially to deal with stiff equations.

The immediate result was that we had no predicted flame temperatures to guide the radiation modeling described below, and had to rely on the analysis of spectral features to derive temperatures. The long term outlook for flowfield modeling encompasses two possibilities. It may be that modifications to BOAT will result in a useful program, so this should definitely receive some further investigation. Also worthy of further investigation is a good possibility that other existing flowfield and kinetics codes can be integrated and/or developed with sufficiently little additional work that they become useful codes for predicting more realistic flowfields than would ever be given by BOAT.

3.2 Chemical Kinetics Modeling

A major component of a coupled fluid dynamics/chemical kinetics model is the chemical reaction set. Although the flowfield calculation needs additional work, we were able to make some interesting preliminary calculations using a one-dimensional chemical kinetics program.[14] The example reaction set developed in this program was for the combustion of the BAMO/NMMO binder with and without boron.

The initial decomposition products of BAMO/NMMO were taken to be CH_2O (22%), C_2H_4 (12%), C_2H_2 (5%), CH_3 (3%), HCN (24%), NO_2 (5%), N_2 (24%), CH (2%), and H (2%). This selection was based on an analogy with nitramine decomposition studies[15] and the constraint that the enthalpy of the decomposition products must equal the enthalpy of the BAMO/NMMO binder. The above species distribution and a mixture temperature of 473 K (which is the burning BAMO/NMMO surface temperature in the Penn State studies[16]) were used as initial conditions for the chemical kinetic calculations for BAMO/NMMO combustion.

The combustion process was first studied using a well-stirred reactor model. The results showing the temporal evolution of species during primary combustion are presented in Figures 20-22. Plots of the major decomposition product species in Figure 20 show that slight changes occur in the mole fractions of CH_2O and NO_2, while the mole fractions of HCN, C_2H_4 and C_2H_2 are virtually unchanged. Plots of the products of primary combustion and the temperature profile given in Figure 21 show that the reactions are essentially completed in 10^{-5} s, with the major products being CH_4, CO, NO, H_2O, and H_2. The history of the combustion radicals, given in Figure 22, shows that O, OH, and HO_2 are consumed in less than 10^{-4} s, while at the same time, NCO and HCO reach relatively high steady state levels. It is evident from Figures 20-22 that the primary combustion process of BAMO/NMMO is severely limited by a lack of oxidizer. Exothermic reactions producing the products shown in Figure 21

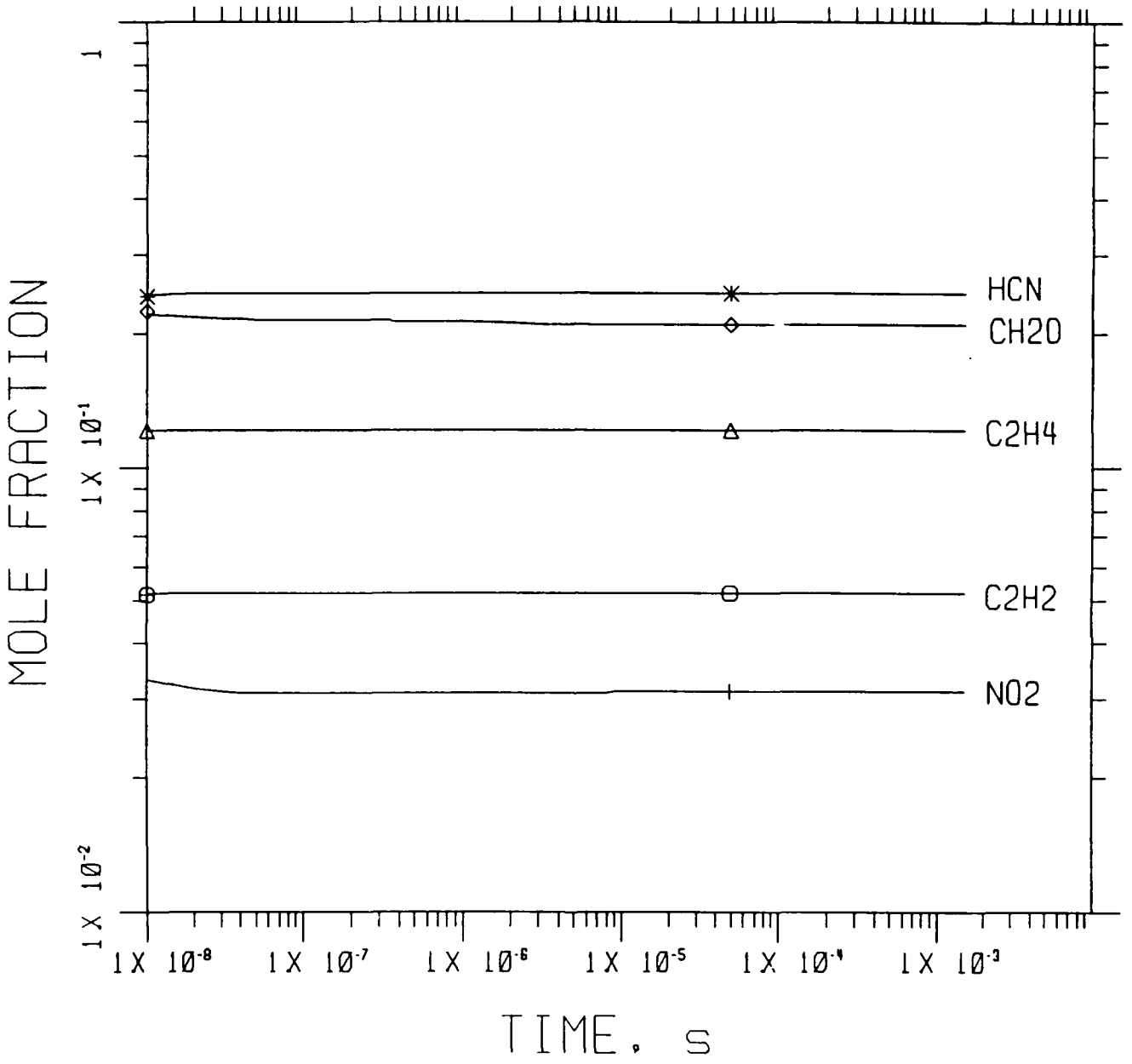

Figure 20. Temporal Evolution of Major BAMO/NMMO Decomposition Product Species.

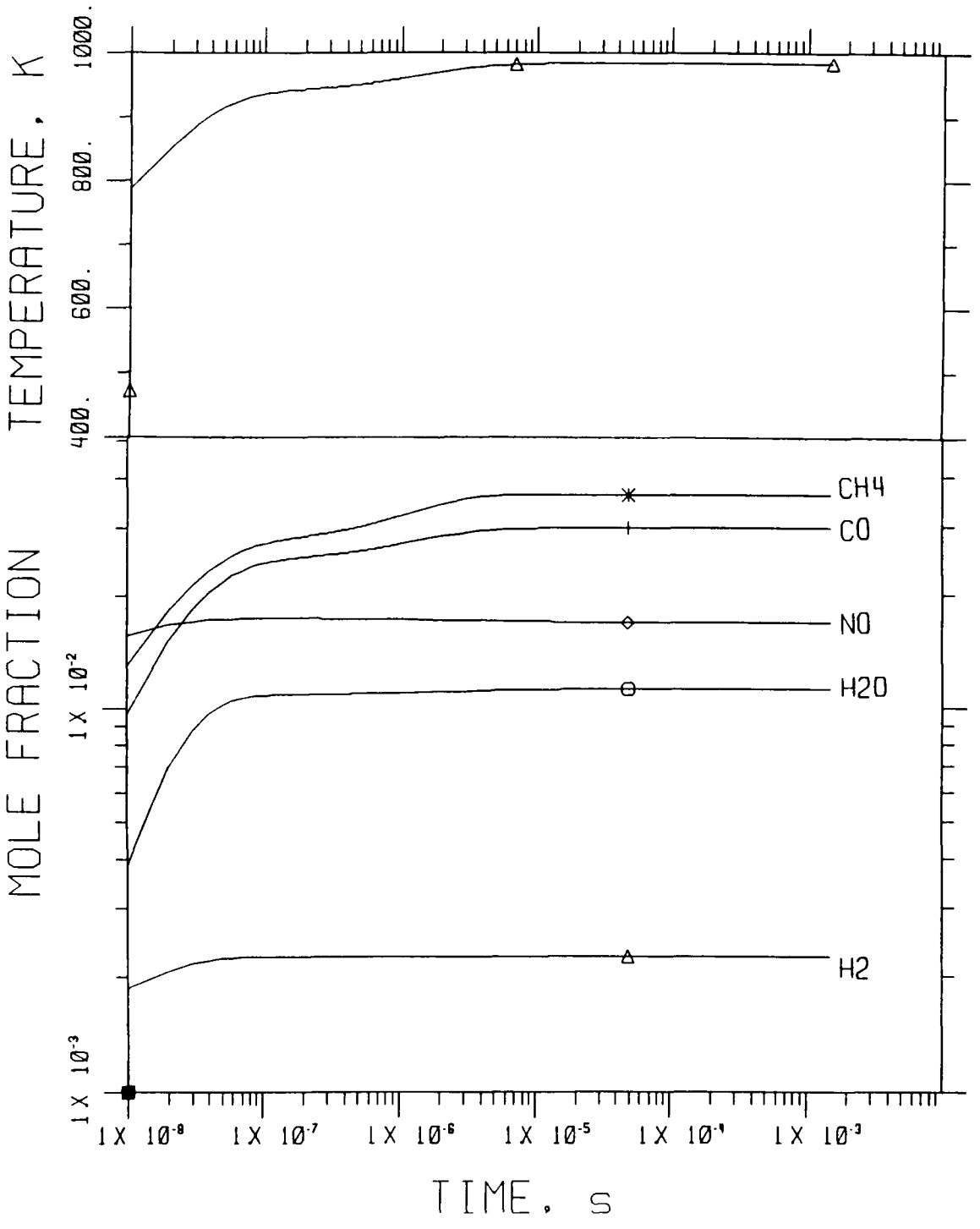

Figure 21. Temporal Evolution of Products of BAMO/NMMO Primary Combustion and Temperature.

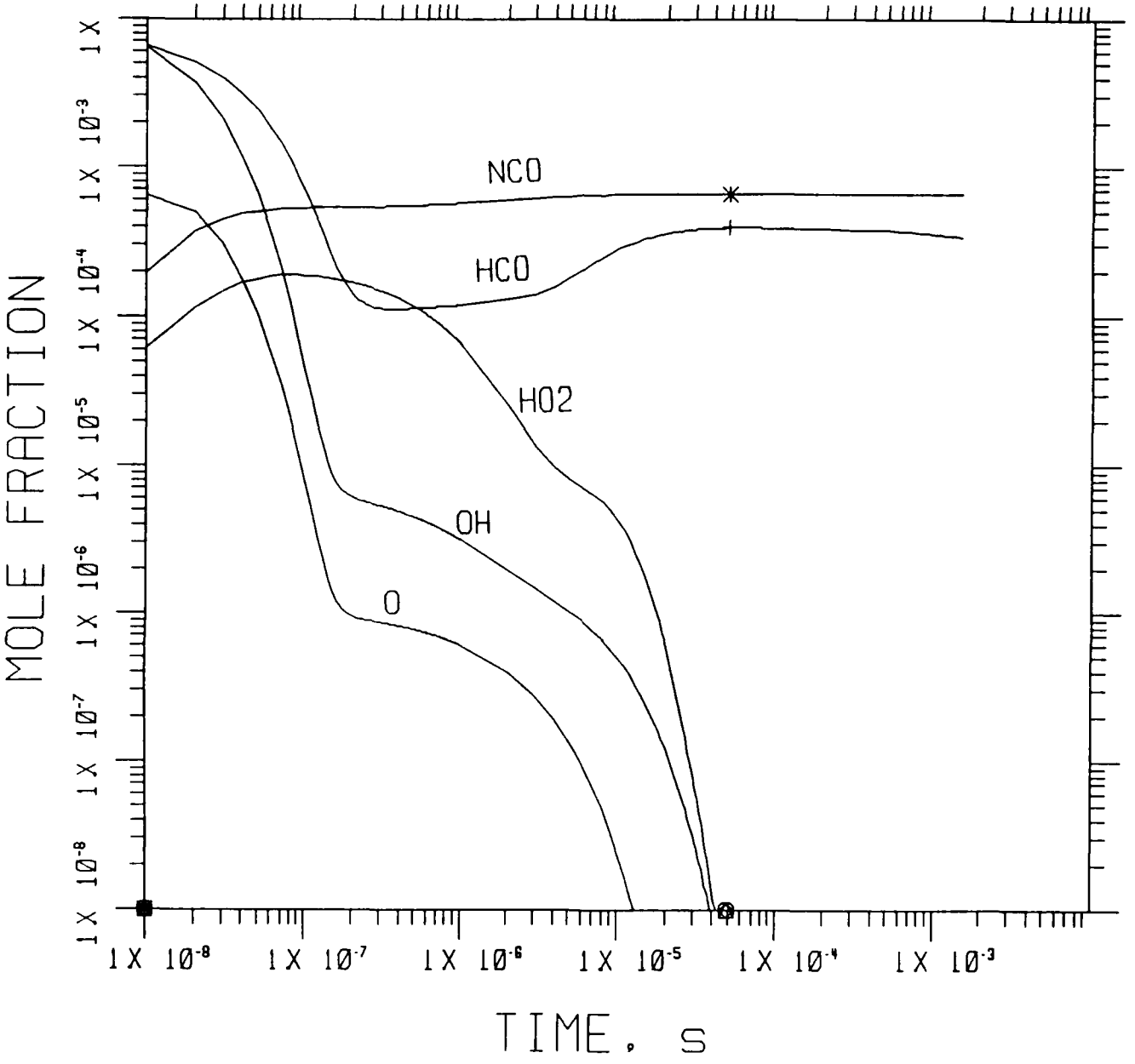

Figure 22. Temporal Evolution of BAMO/NMMO Primary Combustion Radical Species.

raised the mixture temperature only to 980 K. This calculated temperature agrees well with the first stage maximum temperature of 910 K measured for the combustion of BAMO/NMMO with 29% boron at the same pressure of 214 kPa.[16]

The effect of 10% oxygen addition to the primary combustion products is shown by species mole fraction and temperature profiles given in Figure 23. The reaction process proceeds after an incubation time of 10^{-5} s, increasing the mixture temperature to over 1500 K. This calculation, therefore, agrees with the observed behavior of vigorous secondary combustion when BAMO/NMMO is burned in an oxidizing environment.[17]

3.3 Radiation Modeling

Radiation modeling based on the simplest possible model of the emitting region was used in three investigations of the types of information which could be gained by comparison of predictions and observations. These were all preliminary investigations, which could be carried to a higher level of detail with additional effort. In the first, we made comparisons with the spectral shape of a full low resolution spectrum for each of the two propellants burned in air, looking at how accurately temperatures and relative species concentrations (of CO, CO_2 and H_2O) could be determined. The second study looked at determination of NO and H_2CO concentrations in the inert gas burning case, while the third picked a small section of the HCl emission spectrum as an example of our line-by-line modeling capability.

3.3.1 The Radiation Model

Radiation modeling was done using the Aerodyne Radiation Code (ARC), which computes radiation emission and transport from a source consisting of a set of concentric cylinders.[13] The radiating region used to model the flame was a single cylindrical volume with uniform temperature and concentrations, viewed at 90 degrees to its axis. It was surrounded by an annular region

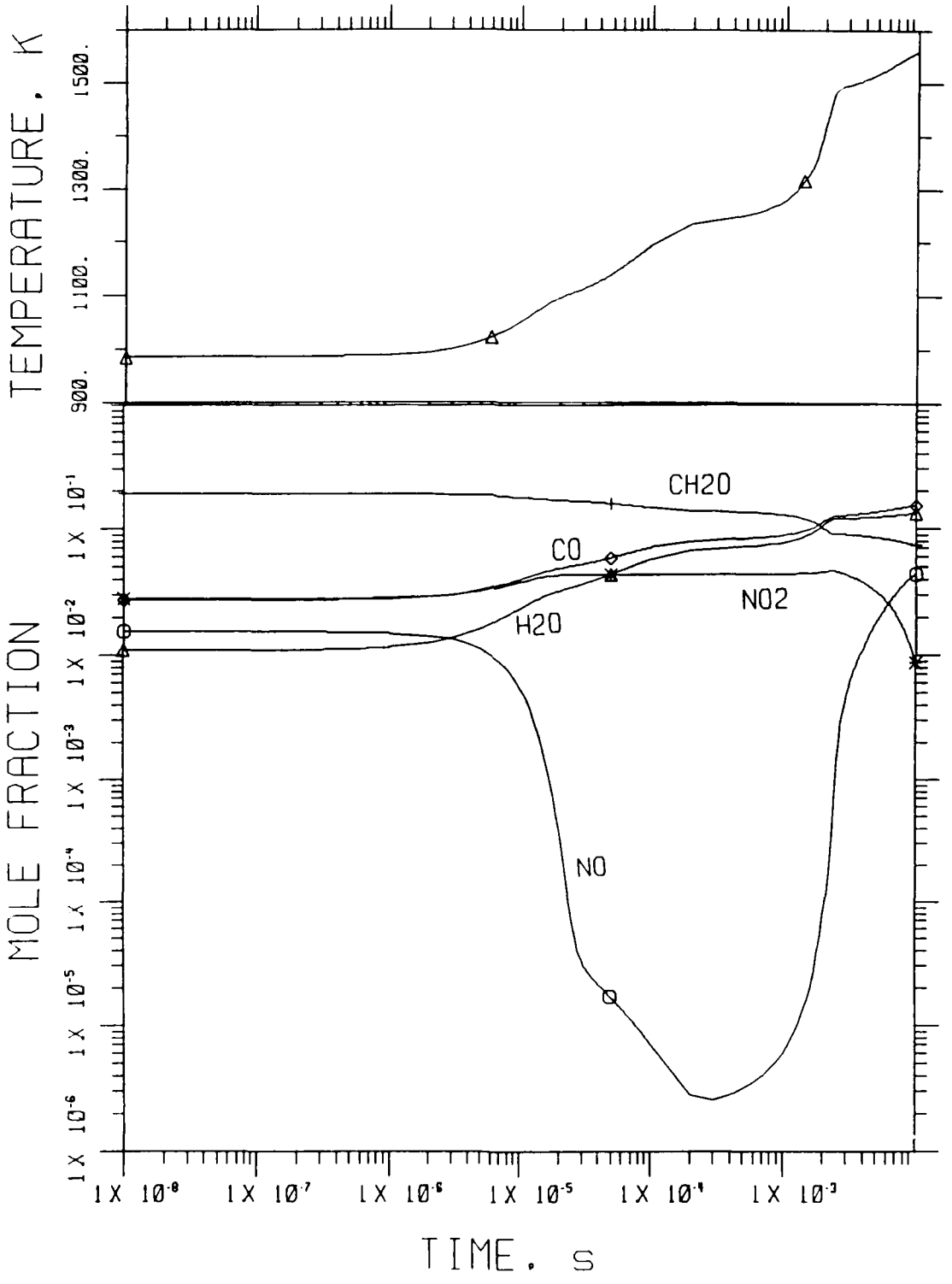

Figure 23. Temporal Evolution of Major Combustion Species and Temperature after O_2 Addition.

which could be used to model cooler, recirculating combustion product gases. In addition, a separate, uniform low temperature region was included in the model, to account for radiation from the hot surface of the propellant.

Figure 24 is the first of two examples of the modeling of the entire low resolution spectrum, showing the comparison with the observation of NOSOL-363 burning in air. In this case, the hot region was given a radius of 1.5 cm and had a 0.75 cm length and a 2000 K temperature. A surrounding annular region was not used, and the additional region used to simulate blackbody emission was given a temperature of 300 K. In addition to the gaseous radiators CO, CO_2 and H_2O, a small amount of soot at the flame temperature was used in the model to supply the continuum radiation observed between molecular bands- in the actual flame this radiation could be due to a variety of particulate sources, or at least in part to the burning surface.

We should point out here that to first order it is neither the dimensions of the radiating regions or their molecular concentrations alone which are being compared with the observed spectra, but their product, called the column density. Although the dimensions cited above are close to the true dimensions of the visible flame, they were chosen before we had video records of the Penn State burns. Our examination of visible flame sizes in these videos suggests that hot region dimensions of 1 cm radius and 3 cm height would be closer to the truth (the truth is, of course, that the hot region is not a single uniform volume but possesses substantial temperature gradients, and these certainly affect the shape of the spectrum, although typically only in a second order fashion).

With all this said, if we continue to report the molecular concentrations appropriate to a model with a 1.5 cm radius hot cylinder, we used mole fractions of 0.15 for CO, 0.22 for H_2O, 0.20 for CO_2, and 0.0012 for soot. If a larger flame radius were used, these mole fractions would be cut by the same factor, and vice versa. In any case, the relative concentrations of the gas

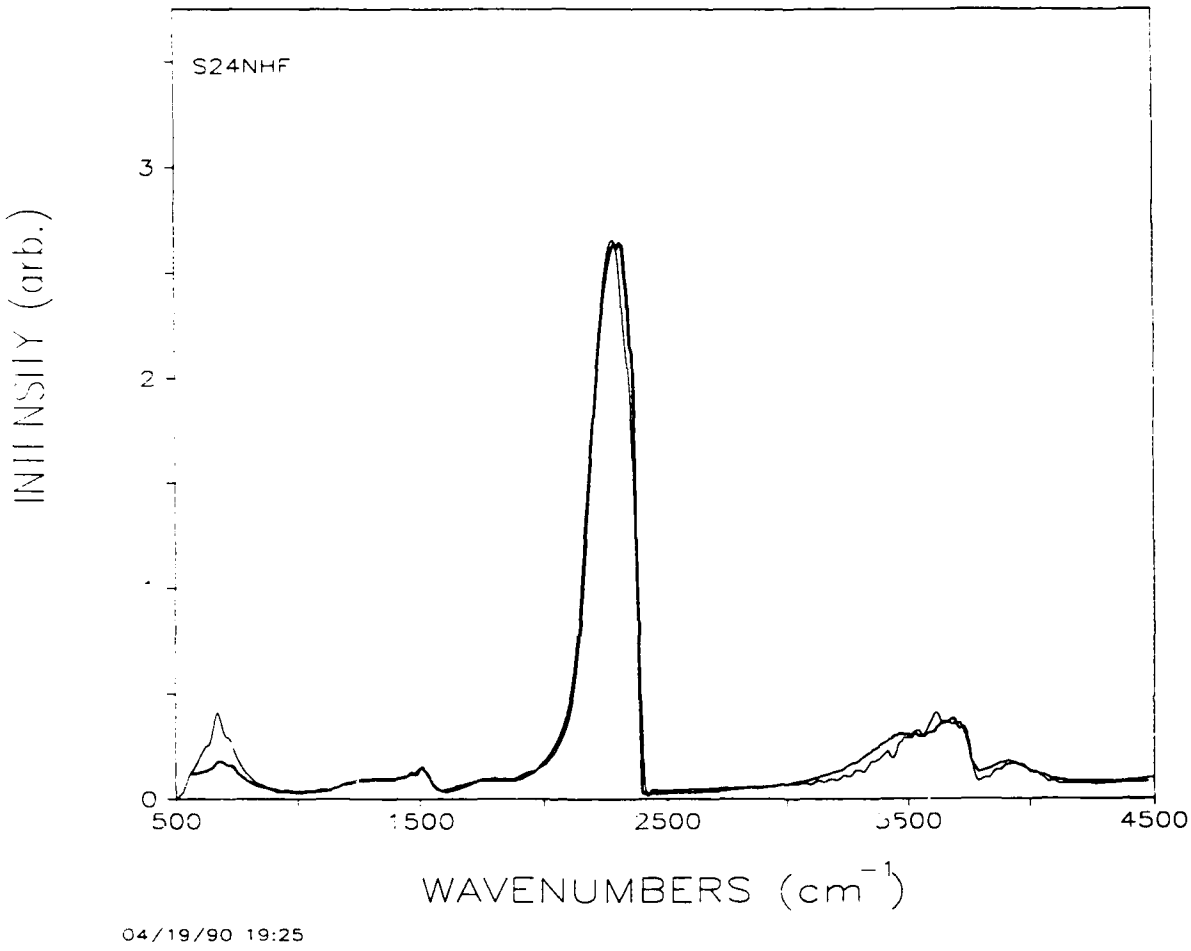

Figure 24. Band Model Radiation Prediction (Heavy Line) Overlaid on Smoothed NOSOL-363/Air Observed Spectrum Reproduced from Figure 11.

phase species are in fact consistent with the formula of the NOSOL-363 propellant.

3.3.2 Band Model Prediction Comparison to NOSOL-363 Spectrum

It can be seen that the agreement in Figure 20 is in general quite good. The largest discrepancy appears in the long wavelength CO_2 band. A discussion of what model changes could be made to decrease this difference will give an indication of how robust the present model is.

If the CO_2 concentration were to be increased to make up the difference, this would have two undesirable effects. First, to maintain the C/H ratio in the propellant, the CO/CO_2 ratio would have to change, and this would give poorer agreement in the CO band region around 2000 cm^{-1}. Second, the optical depth of the mid-wavelength CO_2 band would be greater and its shape would change to one which was broader and blunter than the observation (some of this type of disagreement is already seen). With additional adjustments (such as a small amount of cold gas absorption to narrow the mid-wavelength CO_2 band at its high frequency side) it is possible that an initial increase in CO_2 optical depth in the model could be accommodated with a net result of better overall agreement.

On the other hand, there are other possible explanations for the problem in the long wavelength CO_2 band. In principle, a lower temperature radiator, with its spectral intensity shifted to lower frequencies, would have a better ratio of the two CO_2 bands without changing the CO_2 optical depth. Other changes would be necessary, however. Since the H_2O band around 1500 cm^{-1} would also have a relative increase, the H_2O column density would have to decrease, again a problem if we want to preserve the elemental composition of the propellant in the three combustion product species CO, CO_2 and H_2O. Furthermore, a decrease in temperature will have a noticeable effect on the widths of several bands, including the mid-wavelength CO_2 band and the short

wavelength water band around 3500 cm^{-1}. Indeed, this latter band is narrower (and therefore cooler) in the observed spectrum than it is in the model spectrum. However, a cooler spectrum would be relatively lower here even while being higher in the 1500 cm^{-1} water band, so more adjustments than simply raising or lowering the H_2O column density would have to be made.

At this point it is fair to point out that the use of a model with more than a single radiating region with one uniform temperature might be the way to accomplish several of the seemingly contradictory goals mentioned above, since volumes with both high and low frequency regions of the spectrum enhanced relative to the central CO_2 band intensity could be added to the source. Finally, we cannot rule out the possibility that there is a problem with the calibration spectrum we used relative to the actual spectrometer sensitivity when these spectra were obtained (although the two measurements were made only 3 days apart). It can be seen that the same problem is also the largest discrepancy in our other full band model comparison, with one of the B/BAMO/NMMO/air spectra, shown in Figure 25. Whether this is due to a systematic problem in the data reduction or a systematic problem with the model is difficult to decide at this point.

3.3.3 Band Model Prediction Comparison to B/BAMO/NMMO Spectrum

The largest difference in the models for Figures 24 and 25 is that while we took 2000 K as the average flame temperature for the NOSOL-363 observation, for the B/BAMO/NMMO comparison in Figure 25 the single temperature in the model is only 1400 K. This results in narrower band widths in the mid-wavelength CO_2 and 1500 cm^{-1} H_2O bands, for instance (in both cases, perhaps a little narrower in the model than in the observed spectrum). It also results in a lower ratio of short wavelength to long wavelength water band intensities, in accord with the observation. Although this ratio can be affected by the choice of spectral characteristics of the continuum component of the spectrum (hot particles and hot surfaces may have very different

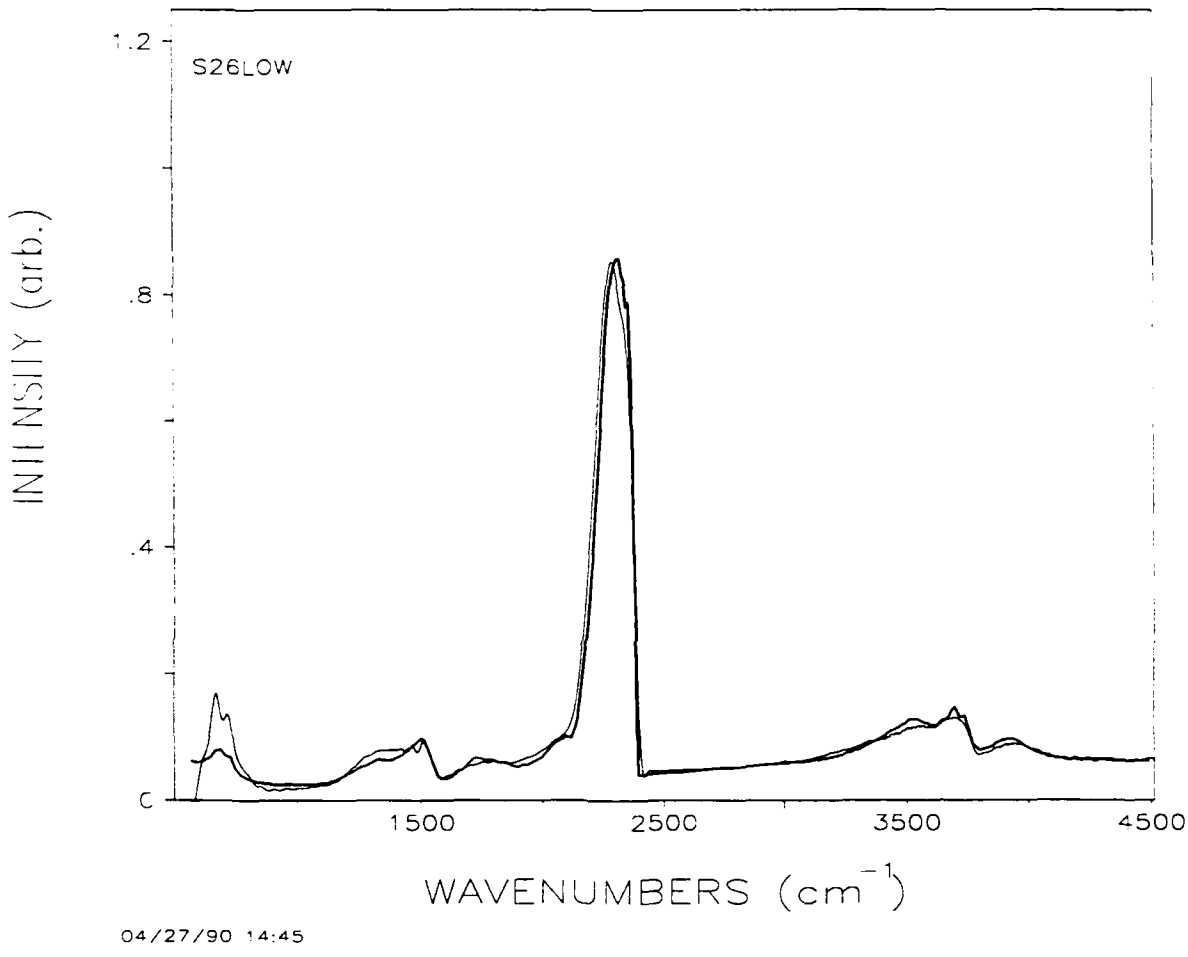

Figure 25. Band Model Radiation Prediction (Heavy Line) Overlaid on Smoothed B/BAMO/NMMO/Air Observed Spectrum Reproduced from Figure 13.

spectra, for instance), on the whole it seemed compelling evidence that the B/BAMO/NMMO flame of Figure 25 is substantially cooler than the NOSOL-363 flame of Figure 24.

The other parameters of the model used to produce Figure 25 include a somewhat smaller cylinder radius, 1 instead of 1.5 cm, and mole fractions of 0.2 for CO, 0.3 for H_2O, 0.2 for CO_2, and 0.007 for soot. Again, these reflect the elemental composition of the propellant. A contribution from a 300 K blackbody was included to raise the long wavelength continuum level- presumably a more realistic model would replace both this contribution and some of the 1400 K blackbody radiation from the soot in the flame volume with blackbody radiation for some intermediate temperature representing the burning surface. However, the combination of 300 K and 1400 K curves seems adequate for a first cut at representing the continuum component of this spectrum, since good agreement is achieved at 1000, 2500, and 4500 cm^{-1}.

3.3.4 Band Model Prediction Comparison to NOSOL-363/N_2 Spectrum

We did not work on a detailed model of the spectra for NOSOL-363 burning in nitrogen, first shown in Figures 2 and 3. However, we were interested in doing just enough to be able to estimate rough column densities for the molecular species which are peculiar to burning in an inert atmosphere, H_2CO and NO.

The H_2CO molecule is a member of the molecular class with the most complicated spectra, that of asymmetric tops. One way to construct a band model for such a molecule involves a two step procedure, in which as asymmetric rotor program[19,20] is used to write a file of predicted line positions and strengths, and then a second program[21] reads this file and averages over the desired resolution to produce the band model. We have used this procedure for other molecules, but for large molecules and high temperatures it becomes tedious to be sure that enough lines have been included.

An alternative which should be more than adequate for our purposes is to approximate H_2CO by a symmetric top with the same value of the largest rotational constant and with a second rotational constant which is the average of the two smaller constants of H_2CO. This approximation has worked well for even more complex molecules[22] and has the advantage that a single program[23] exists which carries the calculation all the way from input molecular constants to a band model suitable for input to ARC. It has the additional feature that hot band contributions are automatically included.

For the H_2CO ν_2 band we were aided by the fortunate circumstances that an asymmetric rotor/band model calculation had been carried out and published,[24] although for 300 K only. We were able to adjust our input parameters to the symmetric top band model code to get good agreement with the published spectrum. Higher temperatures bring out hot band Q-branch features. Their positions have not yet been brought into agreement with those in the Penn State spectra, but we believe we have enough adjustable parameters that this could be done. A recent paper,[8] focusing on intensity measurements of all bands, also reports 300 K absorption observations and calculated band contours at even higher spectral resolution than Reference 24. This paper would be very valuable if we were to go on to make a band model of the overlapped ν_1 and ν_5 bands (which its authors state is not overly complicated by interactions between the two vibrations).

The NO band model we used was (presumably) the one documented in the NASA handbook.[25] This is perfectly adequate to compare with the present data because at 4 cm^{-1} the individual NO lines are not resolved. However, since the NO line spacing is only about 3 cm^{-1}, they could easily be resolved if a 1 cm^{-1} spectrometer resolution were used, and then the line-by-line NO model we developed early in the program could be used to analyze the band profile.

Finally, in this study we used a higher resolution (5 cm^{-1}) H_2O band model[21] than used in the rest of the work reported here. This compares better

with the band shape of the 4 cm^{-1} observations, although agreement is still not perfect. The H_2CO band model is tabulated every 4 cm^{-1}, while the minimum point spacing in the NO band model is 25 cm^{-1}. Better agreement could be obtained by calculating band models (or employing resolution function averaging programs) at the point spacing of the Penn State spectrometer, but for our present purposes, the models we used are adequate.

Figure 26 gives a closer look at one of the inert atmosphere spectra, showing the unknown band centered at 1100 cm^{-1}, then the H_2O band from 1200 to 1600 cm^{-1}, then the H_2CO band (and NO P branch) from 1600 to 1900 cm^{-1}, and finally the NO R branch peaking at 1930 cm^{-1}. To compare with this, we made the band model calculations summarized in Figure 27.

The model parameters for this calculation included a 1.5 cm cylinder radius, a 1000 K temperature (no detailed analysis was made to support this temperature, since errors in temperature should only have second order effects on determination of relative mole fractions), a water mole fraction of 0.22, and mole fractions of 0.2 for both NO and H_2CO. It can be seen that, to first order, the mole fractions of the three molecules must indeed be very similar.

3.3.5 Line-by-Line Prediction Comparison to NOSOL-363 Spectrum

The application of halocarbon grease to the strand observed in runs S23 and S24 gave rise to the happy artifact of strong HCl and HF emission bands. Although the 4 cm^{-1} spectrometer resolution used in these observations is really too coarse to justify detailed modeling of these bands, when higher resolution spectra will no doubt be taken, we were still curious to do a line-by-line prediction for a small spectral region. The region we chose, without any a priori justification, is shown in Figure 28.

This seems to show two HCl lines, but as can be seen in the model prediction of Figure 29, many lines contribute. Only the pair around

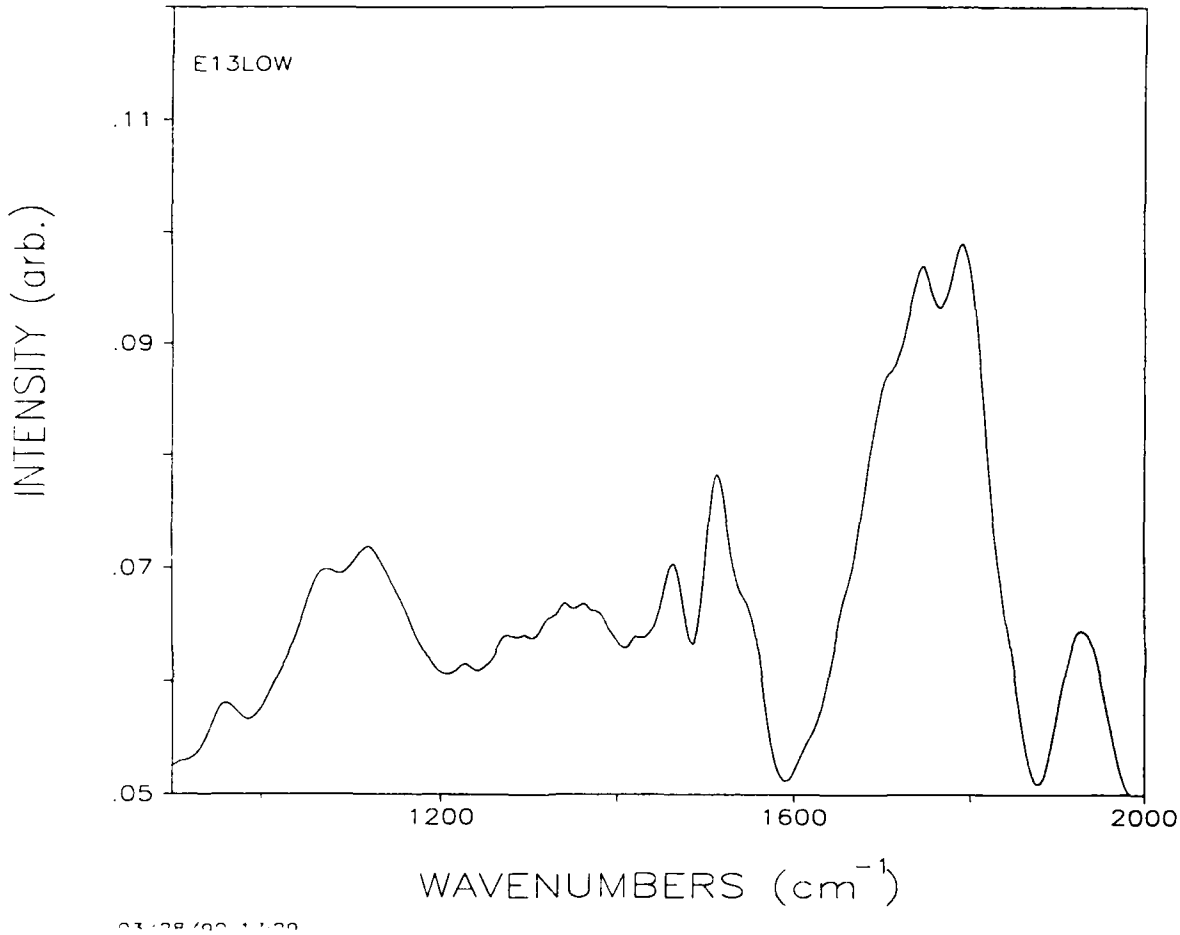

Figure 26. Expanded View of Smoothed NOSOL-363/Nitrogen Specturm Originally Presented in Figure 9, including H_2O, H_2CO and NO Bands.

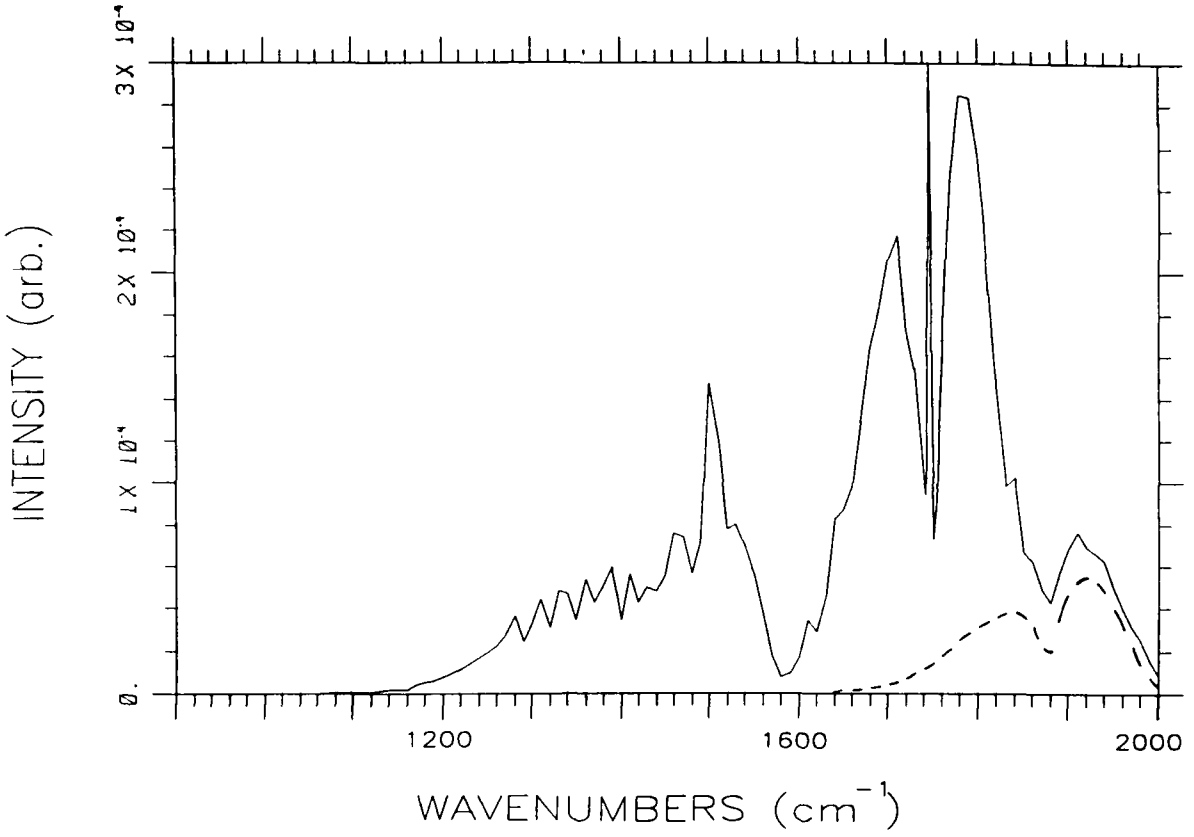

Figure 27. **Band Model Predictions for Comparison with Figure 22. The Dashed Line Shows the Contribution from NO Alone - Most of the Remaining Radiation Above 1900 cm^{-1} is Due to H_2O.**

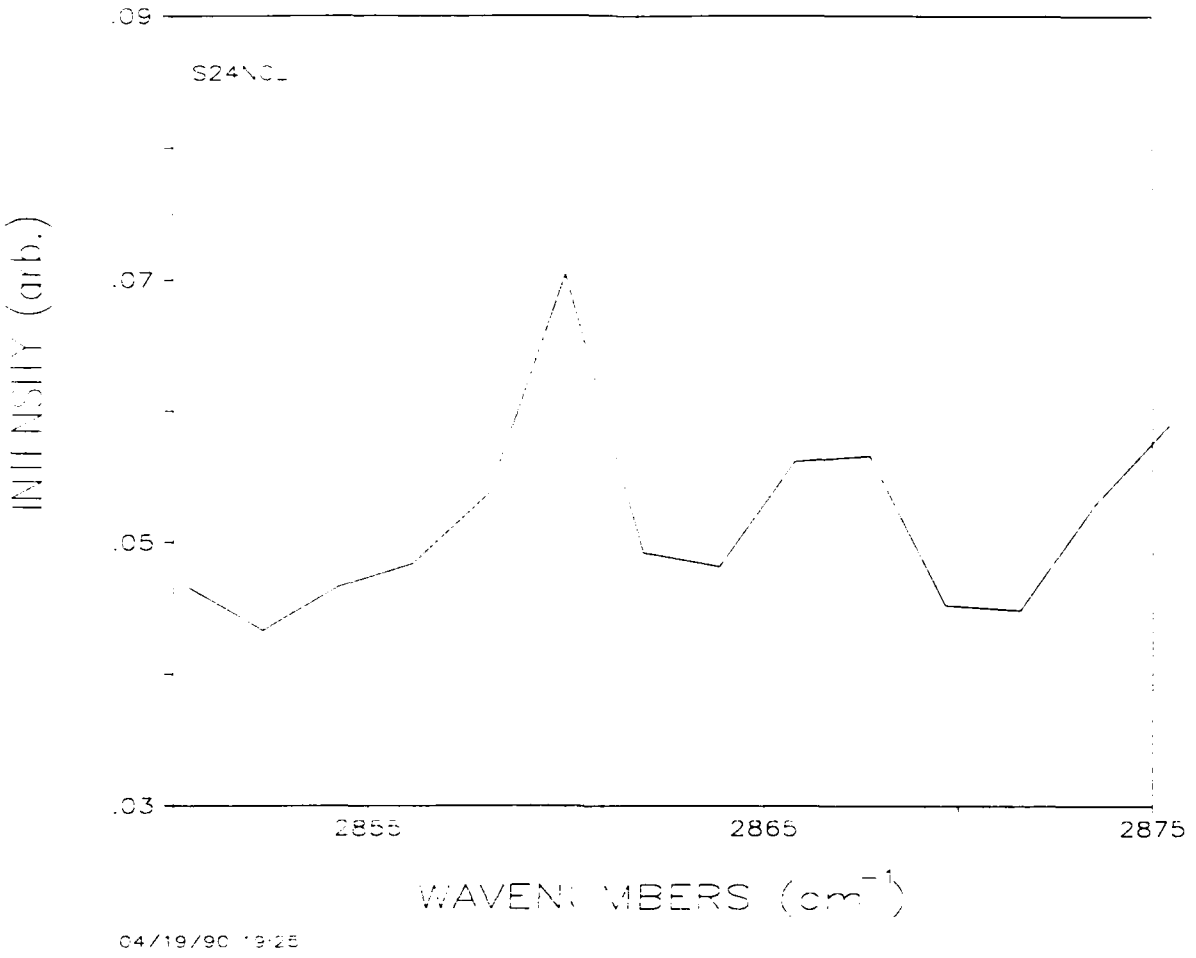

Figure 28. Expanded View of NOSOL-363/Air Spectrum Originally Presented in Figure 5, a Region Containing Partially Resolved HCl Line Emission.

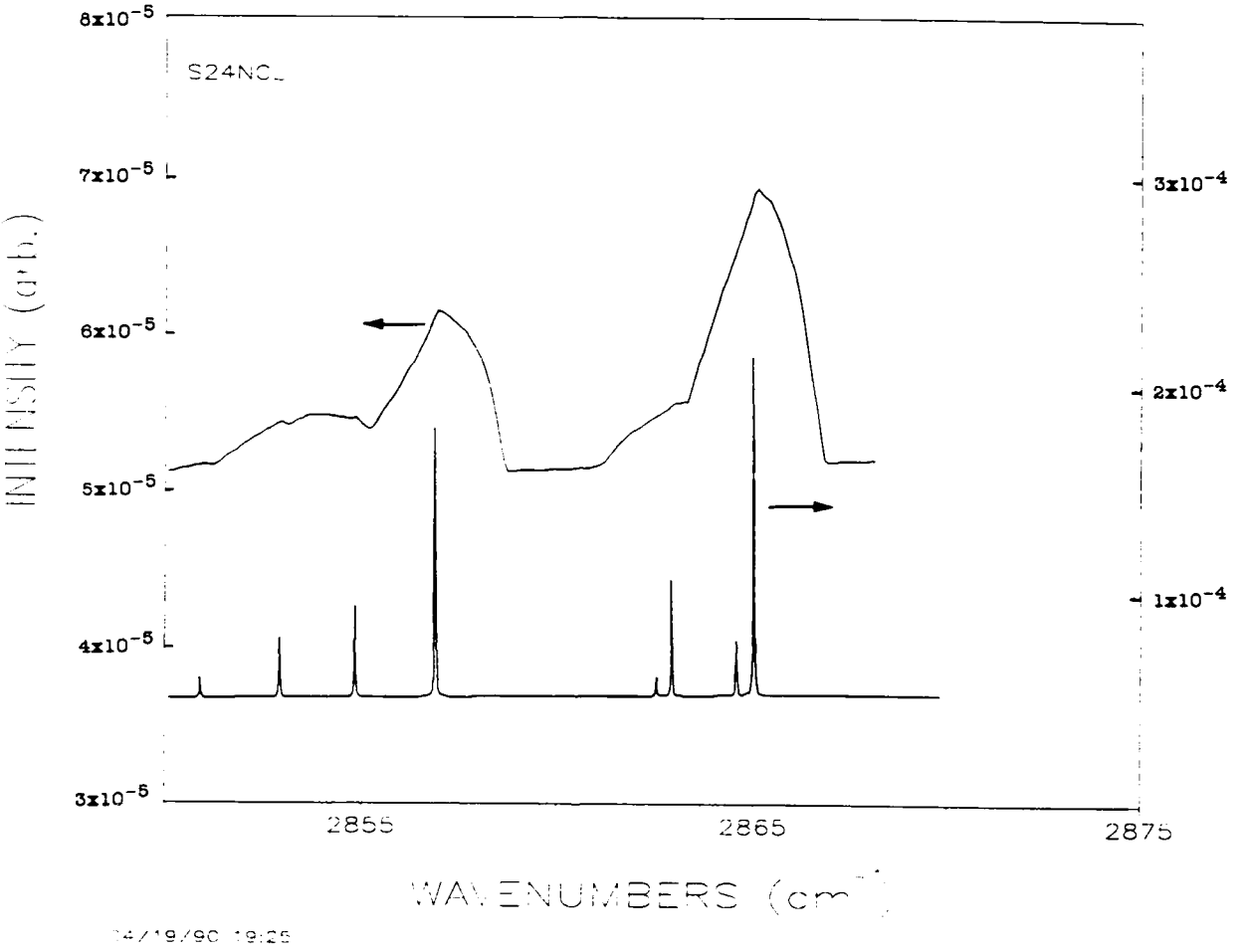

Figure 29. Line-by-Line ARC Prediction of the HCl Emission Region Shown in Figure 24. Lower Curve Shows HCl Emission Lines with Their True Width, While Upper Curve Shows the Result of Applying a Triangular Instrument Function with a 4 cm^{-1} Base.

2865 cm^{-1} (here, the discrepancy between the Penn State spectrometer frequency scale and literature values is apparent) are 1-0 lines (the P(1) line pair)- the rest are due to hot bands, with the pair around 2855 and 2857 cm^{-1} (in Figure 29) being the two isotopic components of a 2-1 transition (the R(3) line pair).

The upper curve in Figure 29 results from the convolution of a triangular instrument function with the HCl spectrum below it. The instrument function has a 4 cm^{-1} base width, intended to approximate the resolution of the Penn State spectrometer. The deviations from triangular shapes are numerical artifacts which could be eliminated by finer grid spacings.

The comparison between Figures 28 and 29 is not as bad as it appears at first glance, because the peak intensity of the right hand (2-1) peak in the observed spectrum has been spread between two points. When areas under predicted and observed peaks are integrated, the difference in 1-0/2-1 ratio is between 1.45 (in the observed spectrum) and 1.75 (in the calculation). A higher resolution spectrum of this region would clearly give a much better representation of the true structure.

4. SUMMARY AND RECOMMENDATIONS

The program to date is perhaps best viewed as an inventory of possible investigation directions. We have had time to look into all the areas which are components of a comprehensive analysis program, but no investigation has yet been carried out with either the depth or breadth needed for the analysis to become a coherent whole which is more than the sum of its parts. Several of the results to date have been very satisfying. More important than the individual results reported so far is our conclusion is that every analysis technique we explored will yield useful information, although some will require substantial additional effort.

We will begin our summary by reviewing the analysis tools developed under this program. Each point will include some comments on the present status and on what development is still required. Some are well developed, some still need considerable work, but in all cases the direction in which to proceed is clear. We can divide the analysis tools into the following areas:

Flowfield modeling- This area needs the most additional work if its is to make a significant contribution. We have several options to pursue, from analytical methods to existing computer codes. The goals here would include independent predictions of flame peak temperatures and of temperature and species profiles, to guide the data analysis techniques used to extract these quantities empirically.

Chemical kinetic calculations- Ideally, these are performed as part of a coupled turbulent mixing/chemistry calculation which accurately represents the flame flowfield. We believe that even in the absence of such a computational capability, one-dimensional chemical kinetics calculations carried out along time/temperature histories resembling those of propellant decomposition products

diffusing and convecting through the flame, can give substantial insight into what species we expect to see from a given mechanism. The work done to date leaves much to be done in the areas of time/temperature histories and of selection of species and reactions, but has demonstrated a worthwhile tool both for data interpretation and reaction set screening.

Species identification by band recognition- At this most basic, qualitative level of spectral analysis, the situation seems fairly well under control for those spectra examined under this program. Of those bands we could see, we had trouble identifying the source of only one, and we claimed to see no evidence of emission from a list of molecules which might have been expected to contribute. Of course, the identity of the unknown may have been under our nose all the time, while spectra of additional molecules may be just below our present noise level or hidden under other bands, waiting for additional work (spectral subtraction, changes in resolution, changes in combustion conditions, for example) to bring them out. Therefore, we can expect additional progress in this area.

Temperature measurement by band model profile matching- This actually comprises two techniques, widths of individual bands, and ratios of pairs of bands of the same molecule. The usefulness of the former technique is easily seen by comparing the greatly differing CO_2 red spike widths for NOSOL in nitrogen and air (Figures 3 and 4). However, comparing the NOSOL and BAMO/NMMO spectra in Figures 5 and 6 the difference is much less obvious, though we believe these flames still have very different temperatures. Use of water band shapes seems to require further analysis, perhaps including the development of more accurate band models. Clearly, this is a technique which presently requires care in

application. The use of relative band intensities also involves careful consideration of potential errors due to continuum contributions and spectrometer sensitivity variations.

Temperature measurement by resolved line peak height analysis- Even with spectra at instrument resolutions which were marginal for the task at hand, this technique produced very promising results. With increases in spectral resolution available with the Penn State instrument, not only HCl and HF but CO and NO bands could be resolved, and cross-checking could put the technique on a solid basis. Even now, we can imagine lowering the uncertainties in derived average temperatures to below 100 K, where the methods reviewed above probably have uncertainties of several times that.

Species concentration determinations by spectral profile matching- In a sense, this is less demanding on the spectral prediction capability than temperature determination, since details of the band shape may be ignored and comparisons made between integrated band intensities to yield concentration measurements of sufficient accuracy that they can be used to evaluate chemical kinetic mechanisms. Of course, a knowledge of temperatures and of temperature and species profiles is needed to obtain truly accurate species concentrations. This task draws on all the other areas, and stands to benefit from any progress in other tasks.

Analysis tools are best developed by comparison to observations, so the above list certainly implies a set of additional analytical investigations we think are worth pursuing. To close, we will list some specific opportunities for new analysis work:

Spectra under conditions which support boron particle burning- Penn State observations include unmistakable evidence of boron particle burning at pressures of 50 psia, while the present test cell had the design goal of operating to 30 psia. It certainly seems worth the effort to reach conditions which produce temperatures high enough for boron particles to ignite. We already have the band models needed to model some of the most likely molecular combustion products, and more progress can be made once some observations are available.

Higher resolution spectra- As mentioned above, higher resolution will allow line-by-line analysis of CO and NO bands as well as HCl and HF. It may well increase the sensitivity to molecular concentrations in several regions of overlapping bands. Higher resolution scans of a wide variety of propellants and combustion conditions, perhaps coupled with additional scan averaging to improve the signal-to-noise ratio, should produce spectra with a significantly higher information content.

Spectral subtraction to reveal hidden bands- This technique, mentioned in connection with possible ways to identify the unknown band in the NOSOL/inert gas spectra, is by no means guaranteed of success, since it requires an excellent knowledge of the shape of the largest bands in the spectrum. It may be that this knowledge will be best gained from a combination of theoretical band modeling techniques and the gathering of empirical reference spectra, for instance in the hot cell now being constructed at Penn State (see below).

Analysis of hot cell calibration spectra- From the several comments about changes in molecular band shapes at high temperatures which are scattered through this report, it should be clear that the

experimental capability to take spectra of pure compounds at elevated temperatures is very important to successful data analysis. Penn State has begun construction of a cell which initially will reach temperatures of up to 1000°C, and with additional work might go as high as 1700°C. The information from these spectra will be most useful if they are used as inputs to band modeling programs which will allow extrapolation of the shapes to any flame temperature.

Comparison of emission and absorption spectra- The emission spectra on which this report has focused contain information about molecular concentrations in the hot regions of the propellant flames. Spectral shapes are sometimes clearly influenced by absorption due to cold gases surrounding the hot flame. Contributions to absorption spectra are not weighted by the blackbody intensities for the temperatures of the gas volumes involved, but rather sample gas concentrations over the entire line of sight. Clearly, the analysis of both types of spectra for the same strand burn would provide more information than either alone. Penn State is developing a capability to switch between the two measurements in consecutive scans using a chopper. We have the capability to analyze absorption as well as emission, and consider this to be a useful avenue of investigation.

Use of small apertures for flame profiling- Penn State now has the capability of using a 1 mm diameter aperture to restrict the size of the volume of the flame which is imaged into the FTIR spectrometer. It is very possible that the accumulation of enough effectively line-of-sight data will allow derivation of temperature and concentration profiles, using inversion techniques. We have used such methods in the past, and would be happy to assist in the analysis of such data sets.

5. REFERENCES

1. A. Savitzky and M. J. E. Golay, Anal. Chem. 36, 1627 (1964).
Y. Oyumi and T. B. Brill, Comb. Flame 62, 213 (1985).

3. R. D. Shelton, A. H. Nielsen and W. H. Fletcher, J. Chem. Phys. 21, 2178 (1953).

4. D. E. Milligan and M. E. Jacox, J. Chem. Phys. 41, 3032 (1964).

5. M. E. Jacox, J. Phys. Chem. Ref. Data 17, 269 (1988).

6. T. Shimanouchi, Tables of Molecular Vibrational Frequencies, NSRDS-NBS Publication 39, 1972.

7. C. J. Pouchert, The Aldrich Library of Infrared Spectra, Aldrich Chemical Company, Milwaukee, WI, 1975.

8. T. Nakanaga, S. Kondo and S. Saeki, J. Chem. Phys. 76, 3860 (1982).

9. R. H. Pierson, A. N. Fletcher, and E. S. Gantz, Analyt. Chem. 28, 1218 (1956).

10. D. S. Erley and B. H. Blake, Infrared Spectra of Gases and Vapors, The Dow Chemical Company, Midland, MI, March 1965.

11. E. T. Arakawa and A. H. Nielsen, J. Mol. Spec. 2, 413 (1958).

12. L. A. Gross, P. R. Griffiths, and J. N.-P. Sun, in Infrared Methods for Gaseous Measurements, Ed. J. Wormhoudt, Marcel Dekker, New York, 1985, p. 81.

13. S.M. Dash and H.S. Pergament, "A Computational Model for the Prediction of Jet Entrainment in the Vicinity of Nozzle Boattails (The BOAT Code), NASA CR-3075, 1978.

14. R.J. Kee, J.A. Miller, and T.H. Jefferson, Sandia National Laboratories Report SAND80-8003 (1980).

15. C.F. Melius and J.S. Binkley, "Thermochemistry of the Decomposition of Nitramines in the Gas Phase," Twenty-first Symposium (International) on Combustion, The Combustion Institute, 1953 (1986).

16. W.H. Hsieh and K.K. Kuo, "Combustion Behavior of Boron-Based DAMO/NMMO Fuel-Rich Solid Propellants," presented at AIAA/ASME/SAE/ASEE 21st Joint Propulsion Conference, Monterey, CA, July 1989.

17. W.H. Hsieh, Private Communication, 1989.

18. L. S. Bernstein, J. Wormhoudt, and J. A. Conant, "The Aerodyne Radiation Code (ARC): Physical Assumptions and Mathematical Approximations", Aerodyne Research, Inc., Report No. ARI-RR-183., (1979).

19. S. Carter and L.O. Halonen, Program ASYMVIB, Spectrochim. Acta 41A(9) (1985), software survey section.

20. A.G. Maki, Program ASYMBD7, Private Communication, 1984.

21. D.C. Robertson, L.S. Bernstein and R. Haimes, Aerodyne Research, Inc. Report ARI-RR-232, October 1980.

22. L.S. Bernstein and C.E. Kolb, J. Chem. Phys. 71, 2828 (1979).

23. C.E. Kolb et al. Aerodyne Research, Inc. Report ARI-RN-97, September 1977.

24. T. Ueda and T. Shimanouchi, J. Mol. Spec. 28, 350 (1968).

25. C.B. Ludwig, W. Malkmus, J.E. Reardon and J.A.L. Thompson, Handbook of Infrared Radiation from Combustion Gases, NASA SP-3080, 1973.